Journal of Power Sources 501 (2021) 230001

Contents lists available at ScienceDirect

Journal of Power Sources

journal homepage: www.elsevier.com/locate/jpowsour

A review of air-cooling battery thermal management systems for electric and hybrid electric vehicles

Gang Zhao [a], Xiaolin Wang [a,*], Michael Negnevitsky [a], Hengyun Zhang [b]

[a] School of Engineering, University of Tasmania, Hobart, TAS, 7001, Australia
[b] School of Mechanical and Automotive Engineering, Shanghai University of Engineering Science, 333 Longteng Road, Songjiang, Shanghai, 201620, China

HIGHLIGHTS

- The air-cooling Battery Thermal Management Systems (BTMS) for EVs & HEVs was reviewed.
- Pros and cons of using Lithium-ion batteries in EVs and HEVs were discussed.
- Risks and accidents of thermal runaway of Lithium-ion batteries were examined.
- Design optimization techniques for improving BTMS performance were evaluated.
- Future research direction and potential solutions for air-cooling BTMSs were proposed.

ARTICLE INFO

Keywords:
Electric vehicles
Lithium-ion battery
Air cooling
Battery thermal management system
Review

ABSTRACT

Battery Thermal Management System (BTMS) is critical to the battery performance, which is important to the overall performance of the powertrain system of Electric Vehicles (EVs) and Hybrid Electric vehicles (HEVs). Due to its compact structure, high reliability, and safety characteristics, the air-cooling BTMS has been widely used in EVs and HEVs industry with cost-reduction demand or under severe and unpredictable working environments. This paper first reviews battery heat generation mechanisms and their impact (e.g. thermal aging, thermal runaway and fire accident) on the powertrain system in EVs and HEVs. Then the basic air-cooling BTMS design is reviewed, and a variety of novel design improvements is evaluated to explore the benefits and challenges of the use of the air-cooling BTMS. It is found that with the help of advanced computational numerical simulations and sophisticated experiments, the air-cooling efficiency is greatly improved by introducing new concepts of battery packs, innovative designs of the cooling channel, and novel thermally conductive materials. Based on the review, this paper suggests future research directions and potential solutions in a discussion for further development of the air-cooling BTMS in the EV and HEV industry.

1. Introduction

The greenhouse gases (GHGs) concentration has been growing since the 1900s [1]. The anthropogenic combustion of fossil fuels, especially from the internal combustion engines (ICEs), generates a tremendous amount of CO_2, leading to the GHGs concentration increment in the atmosphere [2]. It is estimated that the total CO_2 emissions by the transport sector in 2018 were about 8258 Mt, contributing to 24.3% of the total world CO_2 emissions [3]. In addition to CO_2, several other gases, such as CO, HC, and NO_X, are all part of the ICE vehicle exhaust tailpipe emissions [4]. As a widely accepted method to reduce GHGs emissions as well as tackle the global warming issues, EVs and HEVs are regarded as the promising substitutions of ICE vehicles by many countries and scientific communities in the near future and are becoming the most dominant forces in global automobile market from a niche market product 20 years ago to an important icon of next-generation transportation [5,6]. The integration of thermal management with the energy storage (battery) component is one of the most important technical issues to be addressed. The onboard battery system is a key component. It is also a heavy, bulky, and expensive automobile component, mostly with a shorter service life than other parts of the vehicle [7]. The battery system usually occupies about three-quarters of the total power train cost of an EV [8,9]. There are four mainstream categories of battery devices for EVs and HEVs [10]: lead-acid battery, nickel-metal hydride battery (NiMH), electric double-layer capacitor (EDLC), and Lithium-ion

* Corresponding author.
E-mail address: Xiaolin.wang@utas.edu.au (X. Wang).

https://doi.org/10.1016/j.jpowsour.2021.230001
Received 9 January 2021; Received in revised form 13 April 2021; Accepted 5 May 2021
Available online 12 May 2021

Nomenclature

A	Battery surface area (m^2)
C_p	Specific heat capacity ($J \cdot kg^{-1} \cdot K^{-1}$)
$\overline{C_p}$	Mean specific heat capacity ($J \cdot kg^{-1} \cdot K^{-1}$)
h	Heat transfer coefficient ($W \cdot m^{-2} \cdot K^{-1}$)
I	Cell current (A)
k	Thermal conductivity ($W \cdot m^{-1}\ K^{-1}$)
m	Cell mass (kg)
q	Heat transfer rate ($W \cdot m^{-3}$)
$R_{j,total}$	Adjusted battery post's resistance (Ω)
R_o	Ohmic resistance (Ω)
R_p	Polarization resistance (Ω)
T	Absolute cell temperature (K)
V	Cell potential (V)
$U_{l,avg}$	Reaction l's theoretical open circuit potential (V)

Greek symbols

α	Constant
ρ	Cell density ($kg \cdot m^{-3}$)

Subscripts

amb	Ambient
avg	Average value
l	Reaction l
m	Mean value
OC	Open circuit
x, y, z	Three coordinate axis directions

Abbreviations

ARC	Accelerating rate calorimeter
BTMS	Battery thermal management system
CFD	Computational fluid dynamics
DEC	Direct evaporative cooling
EDLC	Electric double-layer capacitor
EV	Electric vehicle
GHG	Greenhouse house gas
HEV	Hybrid electric vehicle
HVAC	Heating, ventilation, and air-conditioning
ICE	Internal combustion engine
LFP	Lithium iron phosphate
Li-ion	Lithium-ion
MHPA	Micro heat pipe array
NiMH	Nickel-metal hydride
NMC	Nickel manganese cobalt
OEM	Original equipment manufacturer
PEO	Polyethylene oxide
SOC	State of charge

battery. The Lead-acid battery is mostly used as the automobile starting, lighting, and ignition battery. The Nickel-metal hydride battery is firstly applied to the energy power systems for the early commercial EV or HEV models such as GM EV1, G1 Toyota RAV4 EV, Honda EV Plus, and Ford Ranger EV etc. But it is soon substituted by the Lithium-ion battery in almost all the EVs and most of the HEVs. EDLC is a kind of supercapacitors. Due to its fast charging ability and long lifetime, it is usually adopted as the braking energy recover and storage device by most EV and HEV OEMs. Toyota Yaris and PSA Peugeot Citroen even use EDLCs to obtain rapid power boost in their fuel-saving systems. The pros and cons of these four categories of batteries are compared in Table 1.

The Lithium-ion rechargeable battery product was first commercialized in 1991 [15]. Since 2000, it gradually became popular electricity storage or power equipment due to its high specific energy, high specific power, lightweight, high voltage output, low self-discharge rate, low maintenance cost, long service life as well as low mass-volume production cost [16–19]. From Table 1, except for its higher cost than the Lead-acid and NiMH battery, the Lithium-ion battery exhibits the top performance in almost every aspect. Due to these excellent behaviors, the Lithium-ion battery was proven to be the best power source for EVs and HEVs by Sato N [20]. In some cases, they were even considered as the only energy storage or power solution to EVs and HEVs because they could be safely scaled up for any suitable size usage [21]. Tesla used 2976 pieces of Lithium-ion battery cells for its passenger vehicle Model 3 Standard Range Version [22]. The BMW continued to use Lithium-ion batteries in its next-generation EVs, i4 [23]. Honda revealed its new Lithium-ion battery products for the Honda E Urban EV [24]. One of the Chinese auto giants, Geely Auto, applied the ternary Lithium-ion battery with intelligent Battery Temperature Control Management System in its latest model, Emgrand EV [25]. As the leading EV manufacturer with about 25% market share in Europe, Renault equipped its latest model ZOE with Lithium-ion batteries [26]. Hyundai installed a 64 kW h Lithium-ion polymer battery module on its 2019 EV model, Kona Electric Elite [27]. Another traditional multinational Auto giant, FCA group, started to change its focus from ICE to EV and planned to invest 9 billion Euros in its electrification business [28].

A robust and efficient BTMS is essential for the battery packages of EVs and HEVs to deliver optimal performance and maintain a long service life. It is critical to reduce excessive heat accumulations and avoid the risk of thermal runaway. Lithium-ion batteries generate heat both inside cells as well as in the interconnection positions during charging and discharging, leading to excessive battery temperature rise and temperature nonuniformity. In order to remove the excessive heat in the battery, much research has been conducted to develop an efficient BTMS for EVs and HEVs. Rao and Wang [29] reviewed the development of clean vehicles and high energy power batteries and evaluated various BTMS techniques, especially the phase change material (PCM) BTMSs. However, PCM-based cooling is adversely confronted with low thermal conductivity, additional weight, as well as leakage problems. Wang et al. [30] reviewed the design consideration of BTMSs and briefed four types of BTMS cooling methods including air cooling, liquid cooling, PCM and heat pipe cooling techniques. An et al. [31] reviewed and compared these four types of cooling techniques. It was suggested that the selection of BMTS technology should be based on the cooling demand and

Table 1
Comparison of four mainstream batteries [10].

	Efficiency	Specific energy	Specific power	Voltage output	Self-discharge rate	Cost estimation
Lead Acid [11]	L[a]	L	L	M[a]	L	L
NiMH [12]	L	M	L	L	M	M
EDLC [13]	H[a]	L	H	M	H	H
Li-ion [14]	M	H	M	H	L	M

[a] L - Low, M – Medium, H – High.

applications. Liquid cooling was suggested being the most suitable method for large-scale battery applications at high charging/discharging *C*-rate and in high-temperature environments. A similar review was conducted by Xia et al. [32]. Kim et al. [33] reviewed heat generation phenomena and critical thermal issues of lithium-ion batteries. The different BTMS cooling methods were reviewed and categorized. Except for the air and liquid cooling techniques, this paper also reviewed refrigerant two-phase cooling, PCM based cooling, and thermoelectric element cooling. It reported that the heat pipe system needs extra cooling plates with additional weight and volume to enlarge the contact areas with the battery cells. Liu et al. [34] summarized the development of BTMS systems including air, liquid, boiling, heat pipe and PCM based cooling with a particular focus on the PCM cooling techniques. It was suggested that the improvement of BTMS systems should be focused on the performance and safety enhancement of Li-ion batteries. Different from these review papers, Wu et al. [35] focused the review on the liquid-based BTMS systems with the main emphasis on battery modelling method and thermal management strategies.

Although the above literature reviewed different cooling techniques for batteries used in EVs or other applications, there is still a lack of comprehensive review of air-cooled BTMSs for EVs and HEVs. The air-cooling BTMS is one of the major cooling techniques to make EVs and HEVs more efficient and safer. It is popular in some commercial EV and HEV BTMS applications due to its simple structure and relatively low cost. Recently, Akinlabi et al. [36] reviewed the passive and active air-cooling BTMS techniques and design parameter optimization methods to improve the BTMS system performance. It reported that the forced air-cooling BTMS was promising to provide adequate cooling for high energy density battery systems. Based on the literature [36], in this paper, a comprehensive review of the air-cooling BTMS is conducted. It first investigates battery heat generation mechanisms and their impact (e.g. thermal aging, thermal runaway and fire accident) on the power-train system in EVs and HEVs. Then the basic air-cooling BTMS design is reviewed, and a variety of novel design improvements is evaluated to explore the benefits and challenges of the use of the air-cooling BTMS. These innovative design techniques include the improvements on battery pack layout, cooling channel, inlets & outlets position, novel thermally conductive materials, and secondary cooling channels. The advantages, potentials, and challenges of the application of the air-cooling BTMSs in EVs and HEVs are discussed. Outlooks and suggestions for the future research directions of the air-cooled BTMS are proposed based on the review. It contributes to the future air-cooling BTMS applications in the commercial EV and HEV industry.

2. Battery heat generation mechanism and its impact

2.1. Lithium-ion battery development

Due to its dominant contribution to the rapid development of EVs and HEVs in recent years, The Lithium-ion battery was one of the sensations in the Nobel Prize ceremony in 2019. Professor Akira Yoshino, Professor John Goodenough, and Professor Michael Stanley Whittingham were awarded the Nobel Prize in Chemistry for their works in developing Lithium-ion batteries. The Graphite electrode was firstly explored by the Bell Laboratory as the alternative to the Lithium metal electrode. Meanwhile, $LiCoO_2$ was developed as one of the earliest cathode materials for Lithium-ion batteries [37], followed by $LiMn_2O_4$, Li_2MnO_3, $LiMnO_2$, $LiMn_2O_4$, $LiFeO_2$, $LiFe_5O_8$, and $LiFe_5O_4$. In the 1980s, Lithium-ion polymer batteries were first invented due to the discovery of polyacenic semiconductive materials. Since the 1990s, the Lithium-ion battery was commercialized quickly. Lithium Iron Phosphate ($LiFePO_4$, LFP) and Lithium nickel manganese Cobalt Oxide ($LiNiMnCoO_2$, NMC) were both developed as mature commercial Lithium-ion battery products.

In recent years, more novel cathodes and anodes had been developed to meet more and more demanding requirements for commercial Lithium-ion batteries. $LiCoO_2$ was initially used as cathode material in the late 1970s. Many researchers were focused on exploring alternative materials to replace the layered $LiCoO_2$ system since cobalt was expensive with thermal instability [38]. A comparison of the pros and cons of several mainstream Lithium-ion battery cathode materials is listed in Table 2. The Lithium manganese cobalt oxide battery has a distinctive layered structure of high specific capacity, good cyclability, stable structure, low cost, and efficient kinetics [39]. As a result, the $LiNi_{1/3}Co_{1/3}Mn_{1/3}O_2$ battery is becoming one of the most widely used commercial cathode materials recently. Noh et al. [40] also found that the electrochemical properties and safety performance of the NMC batteries were related to their microstructures and physicochemical properties.

Fan et al. [47] enhanced the cycling stability, thermal stability, and electrochemical performances of the Nickel-rich $LiNi_{0.8}Co_{0.1}Mn_{0.1}O_2$ batteries (NCM811) both at ambient temperatures and elevated temperature of 55 °C by forming the Li_3PO_4 coating layers on the surfaces of NCM811 cathodes via the chemical reaction between H_3PO_4 and Lithium residuals. The modern material and coating technologies could further improve the overall performances of Lithium-ion batteries. In the latest study, Jin et al. [48] coated Aluminium-doped Zinc Oxide on the surface of Lithium-titanate anodes ($Li_4Ti_5O_{12}$) and achieved better electrochemical performance when the battery was operated at 0.1–3.0 V. Han et al. [49] synthesized silicon suboxide carbon (SiO_x/C) composite spheres using special heat treatments to a liquid mixture of Hexane and Polydimethylsiloxane. The composite spheres were made of free carbons and evenly distributed SiO_x molecules, which increased the electrical conductivity and volume change tolerances. The Lithium-ion cells with this unique anode showed excellent cycling stability, high rate performance and specific capacity. Yu et al. [50] adopted a capillary drying method to synthesize a compact holey-graphene mesopore-oriented framework combining with $Li_4Ti_5O_{12}$ particles to obtain an optimal balance between sufficient porosity for the fast Lithium-ion diffusion and high tap density. The experimental results showed that the high volumetric power materials delivered excellent high rate performance as well as cycle stability. Besides the electrode material enhancement, the physical properties such as dimensions could also be optimized to obtain safer electrodes with a higher specific capacity. Sotomayor et al. [51] produced ultra-thick ceramic $Li_4Ti_5O_{12}$ cathodes and $LiFePO_4$ anodes using a powder extrusion moulding method. The thicken electrode design was proven to achieve a higher gravimetric energy density with low manufacturing cost. Li et al. [52] prepared ultrathin carbon N/S co-doped nanosheets by a facile method as the battery anodes. The novel electrode materials delivered high reversible capacity, stable cycling performance, and good rate capability.

Battery separators and electrolytes are also the targets to improve the Lithium-ion battery performance in recent studies. Shi et al. [53] explored a composite quasi-solid gel separator made of polymer and ceramic particles to strengthen the thermal stability and mechanical property of the separator. Although the uneven ceramic distributions undermined its overall performances at some level, the novel separator exhibited advanced cycling stability and output performance within the wide temperature range from room temperature to about 80 °C. It delivered stable Lithium-ion flow and decreased the rate of Lithium metal dendrite growth rate. Oh et al. [54] developed a three-dimensional separator coated with carbon fibres using a green and economic polydopamine treatment process. The issues of the Lithium metal anode morphological changes were solved by the novel 3D structure of the conductive coatings on the carbon fibre separators. Both the rate capability and cycling performances of the $LiMn_2O_4$/Graphite cells with this new separator were greatly improved compared with the conventional Polyethylene separators, especially the open-circuit voltage behaviour at high temperature (140 °C). Nair et al. [55] proposed an innovative room temperature ionic liquid-based material as the Lithium-rich Nickel Manganese Cobalt Oxide battery polymer electrolyte. The Lithium polymer cells with this high ionic conductivity

Table 2
Comparison of several typical Lithium-ion battery cathode materials.

Material	Specific energy	Ease of preparation	Good *C*-rate capacity	Long cycle life	Thermal stability	Electrical conductivity	Diffusion coefficient	Theoretical capacity	Cost
$LiCoO_2$ [41]	H	H	H	H	L	H	H	H	M
$LiMn_2O_4$ [42]	M	–	–	L	–	M	M	L	L
$LiFePO_4$ [43,44]	M	–	–	–	–	L	L	M	H
$LiNi_{0.8}Co_{0.15}Al_{0.05}O_2$ (NCA) [45]	H	H	H	H	–	–	H	H	H
$LiNi_{1/3}Co_{1/3}Mn_{1/3}O_2$ (NMC) [46]	L	–	H	H	H	–	M	H	L

*L - Low, M – Medium, H – High.

electrolyte and high-voltage cathodes exhibited an extraordinary non-flammability property, excellent cycling performances, good degradation resistance, high oxidation stability and conductivity.

Although Lithium-ion batteries are the dominant products on the current energy storage market, some researchers also focused on other promising ion-based batteries such as Potassium-ion, Sodium-ion, and Zinc-ion batteries. Peng et al. [56] explored a novel Potassium-ion battery cathode manufacturing process for producing P_3–$K_{0.5}MnO_2$ hollow submicron spheres cathode. The 2-step self-templating strategy was scalable and could improve the Potassium-ion storage performance as well as the cycling stability. Wang et al. [57] investigated a novel O_3–$Na(Cr_{0.8}Mn_{0.2})O_2$ cathode material for Sodium-ion batteries, delivering higher average voltage and better cation order without toxic Cr^{6+} formations. A longer Sodium-ion battery life was ensured by the novel low strain cathode structures during the Sodium-ion insertion and extraction processes, showing the potentials of Sodium-ion batteries to be a strong candidate for future energy storage systems. Zinc-ion batteries exhibited superiorities of both high safety and low manufacturing cost due to their less active element property, non-flammable aqueous electrolytes as well as high crustal abundance [58]. Chen et al. [59] presented a promising Zinc-ion battery cathode by fabricating a nanostructure through a fast hydrothermal reaction assisted by facile microwaves. The novel $(NH_4)_2V_6O_{16}{\cdot}1.5H_2O$ cathode exhibited excellent reversible cycling performances due to the large interplane clearance as well as the high diffusion coefficient. For these promising novel ion-based batteries, many fundamental technical obstacles are still needed to be overcome to realize the successful commercialization for the EV and HEV industry.

2.2. Lithium-ion battery heat generation mechanism

In general, the heat generation of the Lithium-ion battery is caused by reaction heat, electrode overpotentials heat, and Joule heat of internal electrical resistance during charging and discharging processes [60]. The heat generation rate is mostly related to the battery operation conditions such as state of charge (SoC), battery temperature, and operation current rate etc. Bernardi et al. [61] simplified the general energy balance equation specifically for the LiAl/FeS cell using an average heat capacity as well as omitting the terms of phase change and enthalpy-of-mixing in Eq. (1):

$$q = I \cdot V + \sum_l I_l \left[T^2 d\frac{\frac{U_{l,avg}}{T}}{dT} \right] + m\overline{C_p}\frac{dT}{dt} \tag{1}$$

where q refers to the heat transfer rate with the surrounding ($W{\cdot}m^{-3}$), I is the cell current (A), V refers to the cell potential (V), subscript l refers to reactions, T is the absolute cell temperature (K), $U_{l,avg}$ is the reaction l's theoretical open circuit potential (V), m refers to the cell mass (kg), and $\overline{C_p}$ is the mean specific heat capacity at constant pressure ($J{\cdot}kg^{-1}{\cdot}K^{-1}$).

Higher charging and discharging rate produce more heat due to internal resistance [62]. During discharging, most electricity generated by the cell is delivered to the external circuit at low discharging rates (2C or less). More voltage is dissipated by the internal resistance as the discharge rate is increased [63]. To achieve maximum power delivery, discharging current should be around half of the short-circuit current. Inside a large Lithium-ion battery format cell, two primary heat sources are irreversible heat generation rate and reversible heat generation rate, both of which are related to the internal resistance, state-of-charge, and cell operating temperature [32,64]. Feng et al. [65] applied a thermodynamic description model of the Lithium-ion battery proposed by Newman et al. [61,66] to predict temperature patterns during charging and discharging by three terms: polarization heat, entropic heat, and convective heat in Eq. (2):

$$mC_p\frac{dT}{dt} = I \cdot (V_{OC} - V) + I \cdot T \cdot \frac{\partial V_{OC}}{\partial T} + hA(T - T_{amb}) \tag{2}$$

where m refers to the cell mass (kg), C_p refers to the specific heat capacity ($J{\cdot}kg^{-1}{\cdot}K^{-1}$), T refers to the absolute cell temperature (K), I refers to the cell current (A), V_{OC} refers to the open-circuit voltage (V), V refers to the cell potential (V), h refers to the heat transfer coefficient ($W{\cdot}m^{-2}{\cdot}K^{-1}$), A refers to the battery surface area (m^2), and T_{amb} refers to the ambient temperature (K).

Xie et al. [67] improved a three-dimensional thermal model for Lithium-ion pouch cells by integrating two sub-models to predict the battery thermal performances at different ambient temperatures and discharge rates with a relatively small error in Eq. (3):

$$\rho C_p\frac{\partial T}{\partial t} = \frac{\partial}{\partial x}\left(k_x\frac{\partial T}{\partial x}\right) + \frac{\partial}{\partial y}\left(k_y\frac{\partial T}{\partial y}\right) + \frac{\partial}{\partial z}\left(k_z\frac{\partial T}{\partial z}\right) + \alpha\left[I^2\left(R_p(\mathrm{SoC},T,I) + R_o(\mathrm{SoC},T,I)\right) + I \cdot T\frac{dV}{dT}(\mathrm{SoC})\right] + (1-\alpha)I^2R_{j,total} \tag{3}$$

where ρ refers to the cell density ($kg{\cdot}m^{-3}$), C_p is to the specific heat capacity ($J{\cdot}kg^{-1}{\cdot}K^{-1}$), T is the absolute cell temperature (K), k_x, k_y, and k_z refer to the thermal conductivities along with x-direction, y-direction, and z-direction, respectively ($W{\cdot}m^{-1}\,K^{-1}$), when α is 1, Eq. (3) is used to calculate the battery temperature, when α is 0, Eq. (3) is used to calculate the post temperature, I is the cell current (A), R_p is the polarization resistance (Ω), SoC refers to the state of charge, R_o refers to the ohmic resistance (Ω), V refers to the cell potential (V), and $R_{j,total}$ is the adjusted battery post's resistance (Ω).

2.3. Lithium-ion battery heat generation rate

In addition to theoretical modelling and calculations, many studies investigated the actual heat generation rates for different materials under different operating conditions. Kobayashi et al. [68] applied the isothermal calorimeter method to measure the heat generation rates of the battery during charging/discharging. It was found that the heat generation rates were determined by different electrode materials ($LiCoO_2$/Li and Graphite/Li) due to the different amount of reversible heat generated from chemical reactions of $LiCoO_2$ or Graphite. Chen et al. [69] measured the heat generation rates of a 20 A h $LiFePO_4$ prismatic cell at different temperatures (−10 °C, 0 °C, 10 °C, 20 °C, 30 °C, 40 °C) and discharging rates (0.25C, 0.5C, 1C, 2C, 3C). The results demonstrated a general trend that the heat generation rates grew with charging/discharging *C*-rates and declined with increasing temperatures in most cases. The maximum heat generation rate reached 29.93 W at 0 °C and 3C discharging rate. Drake et al. [70] measured both the internal heat and the heat dissipated to the ambient using two-point measurements on the surface and one-time measurement on a drilled battery cell. The highest heat generation rate reached 10.6 W at a discharging 9.6C-rate for a 26,650 cylindrical cell (307 W/L as the volumetric heat generation rate). Zhang et al. [71] compared different heat generation rate measuring methods, founding out that the intermittent current method and V–I characteristics method were more accurate than the energy method for measuring the irreversible heat while the potentiometric method was more accurate than the calorimetric method for measuring the reversible heat according to the simplified Bernardi heat generation model. Wu et al. [72] developed a thermo-electrical model to measure the heat generation rate of a large volume of Lithium-ion pouch cells. The heat flux generated from the cell tab areas, especially the positive tab, was found to be much more than that from the cell core. The results showed that the highest heat generation rate of the positive tab reached 2.55×10^5 W/m^3 while that of the negative tab only reached 1.83×10^5 W/m^3, which was 30% lower. Schuster et al. [73] used conventional equipment, accelerating rate calorimeter (ARC), to measure the heat generation rates of a commercial 40 A h Lithium-ion pouch cell during a range of charging and discharging currents (5 A–40 A). The total heat generated at discharging current of 5 A, 10 A, 20 A, and 40 A was 3.48 kJ, 4.47 kJ, 8.47 kJ, and 14.86 kJ, respectively. The total heat generated at charging current of 5 A, 10 A, 20 A, and 40 A was 2.04 kJ, 4.73 kJ, 7.88 kJ, and 14.53 kJ, respectively. Saito et al. [74] used a calorimetry to observe the heat generation performance of Lithium-ion batteries after long time storage. It was found that the degradation due to the long time storage would exhibit higher heat generation behaviour at a high rate (>1C) charging and discharging. The highest heat generation rate reached 0.083 W at approximately 1C discharging rate. Ye et al. [75] used ARC to obtain the heat generation rates of Lithium-ion pouch cell which were 10.45 W, 25.4 W, and 54.4 W at 3C, 5C, and 8C charging operations, respectively. Xu et al. [76] found that the heat generation rate of 55 A h Lithium-ion battery monomer was influenced by the ambient temperature, SOC, as well as charging and discharging rates. For different SOCs, the average heat generation rates were 6.25 W, 6.87 W, 7.19 W, and 6.51 W at 70%, 80%, 90%, and 100% SOC, respectively. For different charging and discharging processes, the average heat generation rates were 2.31 W, 3.42 W, 5.00 W, 6.51 W, 8.44 W, 12.83 W, and 19.17 W at 0.5C, 0.6C, 0.8C, 1C, 1.2C, 1.5C, and 2C, respectively. Wang et al. [77] used temperature sensors to measure the surface temperatures of a battery cell packed by the insulated cotton and polyurethane foam to estimate the heat generation rates. The heat generation rates were 5.89 W, 47.51 W, and 238.80 W at 1C, 3C, and 5C discharging rates, respectively. Sheng et al. [78] applied a novel calorimetric method to measure the specific heat and heat generation rate of $LiFePO_4$ prismatic battery cells. The experimental results obtained by the novel method showed excellent consistency of the heat generation rate to the theoretical results predicted using the new Bernardi's model with a significantly reduced testing time and cost compared with the conventional Bernardi's method. The research team also extended a similar method to measure the thermal properties of Lithium-ion cylindrical 18,650 battery cells [79]. The experimental results obtained by this non-destructive testing method exhibited high accuracy and simplicity. The comparisons of these research regarding the heat generation rates under different operating conditions are listed in Table 3.

Table 3
The heat generation rates under different operating conditions.

Battery model	Operating conditions	Heat generation
20 Ah $LiFePO_4$ prismatic cell [69]	0 °C and 3C discharging rate	29.93 W
2.6 Ah $LiFePO_4$ 26,650 cylindrical cell [70]	9.6C	10.6 W (307 W/L as the volumetric heat generation rate)
25 Ah large-format Lithium-ion pouch cell [72]	25 °C and 1/3C	2.55×10^5 W/m^3 at the positive tab1.83×10^5 W/m^3 at the negative tab
40 Ah Lithium-ion pouch cell [73]	30 °C and 1C	14.86 kJ during discharging14.53 kJ during charging
450 mAh Lithium-ion 18,650 cylindrical cell [74]	25 °C and 1C	0.083 W
55 Ah Lithium-ion battery monomer [76]	20 °C and 1C discharging rate 20 °C and 100% SOC	6.25 W, 6.87 W, 7.19 W, and 6.51 W at 70%, 80%, 90%, and 100% SOC 2.31 W, 3.42 W, 5.00 W, 6.51 W, 8.44 W, 12.83 W, and 19.17 W at 0.5C, 0.6C, 0.8C, 1C, 1.2C, 1.5C, and 2C
20 Ah $LiFePO_4$ prismatic cell [77]	30 °C	5.89 W, 47.51 W, and 238.80 W at 1C, 3C, and 5C discharging rates

2.4. Thermal aging

Heat generations and excessive accumulations during normal operations of Lithium-ion batteries would cause temperature elevations, leading to extensive degradation and shorten battery service life [80–83]. Battery aging initiated at the most possible places connecting electrodes and electrolyte [84,85]. The battery aging phenomenon could cause high internal impedance as well as fast capacity fading [86,87]. Research showed that the battery degradation rates were almost doubled by every 10° temperature rise [88]. Other battery parameters, including SOC and its variations, charging rate and discharging rate, charging and discharging voltage, and moisture level, all have influences on battery aging [89–93]. A mode of battery active site loss was developed to predict the Lithium-ion battery capacity by the National Renewable Energy Laboratory [94]. The battery overall performance was found to be affected by the heat generation and accumulation during charging and discharging. Feng et al. [95] observed the influences of different temperatures (25, 35, 45, and 55 °C) on the Lithium-ion battery aging rates during cycling operations using an electrochemistry-based electrical model. The Graphite and Lithium–Cobalt-Oxide electrode effectiveness, the maximum capacity of electricity storage, the resistances of the electrode and electrolyte, and Warburgr resistance/capacitance all became more adverse at higher operation temperatures (55 °C). Similar finding was also reported by Gabrisch et al. [96]. In this study, the battery thermal aging formed the crystal structures, lowering the battery discharge capacity. Ramadass et al. [80] revealed that the relationship between the cell internal resistance increment and temperature rise. Zhou et al. [97] found that the low-frequency electrolyte diffusion was the main cause of the battery internal impedance rise during the high-temperature cycling. Except for over-heating, the temperature uniformity was also critical to the battery pack's stability and safety, especially when the battery pack consisted of a large number of cells in-series or in-parallel connection [98]. Unlike the computational simulation which could predict the temperature pattern of each part within the battery module and easily found out the hot spot, the actual BTMS could monitor several critical points or battery

cells within the battery pack using temperature sensors. If the maximum temperature difference between different cells is high, the working condition of the cells without temperature sensors will be compromised. For example, when the monitored cell temperature is 39 °C, which is just within the required operation temperature range of less than 40 °C, the pre-set BTMS active cooling strategy and mechanism will not be triggered according to the battery thermal management program. In this specific scenario, the maximum temperature difference of the BTMS is 10 °C which means some battery cells probably have temperatures reaching 49 °C without any active cooling. According to the research, 49 °C will accelerate battery degradation and shorten its service life. In addition, if the specific high temperature cell always lacks cooling, it will probably be the first onset of thermal runaways and cause fire accidents. On the other hand, different operation temperatures will lead to different output performances such as voltage, current, and internal resistance, which will finally influence the whole battery module's stability and output performance. Ni et al. [99] agreed that the reliability, cycle life, electrochemical characteristics, and safety of the cylindrical battery cells pack will be seriously affected by the temperature nonuniformity of all its cells. As a result, {Zhou, 2019 #2725}a temperature range of 25–40 °C and a maximum temperature difference of 5 °C were recommended as the optimal Lithium-ion battery charging and discharging temperatures [100–105]. Schmidt et al. [106] suggested that the batteries might suffer no more aging during high rate discharging than during low rate discharging if they are sufficiently cooled down.

2.5. Thermal runaway and fire accidents

The extreme case of excessive heat accumulation is battery thermal runaway. Its risk would be very high at over-elevated temperatures, causing fire or explosion accidents [107,108]. Excessive heat accumulation mainly came from Joule heat created during the charging and discharging processes [109]. If the unwanted heat could not be removed effectively, it would gasify battery components such as electrolytes and separators, rocketing the cell temperature by several hundred degrees within just a few seconds [110]. Barkholtz et al. [111] investigated the Lithium-ion battery component materials during the battery thermal runaway processes. The collected data proved that the exothermic solid-electrolyte interface and anode decomposition was the main cause for battery self-heating. The decomposition energy melts the separator, triggering the internal thermochemical reactions and short circuit. A tremendous amount of high-pressure gases contained in a small cell would result in fatal ignition and burst [112,113]. In addition, some researchers indicated that the sudden explosion of electrolytes was potentially toxic to the people in an enclosed space such as car cabin [114,115]. The disastrous thermal runaway accidents could cause significant economic losses to OEMs by the unlimited compensations paid to the sufferers as well as the corresponding large-scale recall or withdrawal costs [116,117]. Pfrang et al. [118] reviewed some international battery standards and regulations such as ISO 12405 and IEC 62660 and summarized the most common test conditions for battery safety assessment: mechanical abuse condition, electrical abuse condition, and thermal abuse condition. Feng et al. [119] found that the OEM's intensive cost reduction activities and battery energy density upgrade in recent years have aroused more and more battery thermal runaway accidents which could be classified into thermal abuse conditions. The consequences of ineffective battery temperature management can be tragic [120]. As a result, a reliable and effective battery cooling system with suitable equipment and mechanism is crucial to eliminate safety issues such as thermal runaways and explosions [121–123].

3. Air-cooling BTMS

The EV and HEV battery thermal management is critical to the battery pack to achieve ideal output performance as well as to extend service life during normal operations in different climate conditions [124,125]. Although the ideal operation window for a Lithium-ion battery is a relatively narrow range from 25 °C to 40 °C, the actual operating temperatures could be from −30 °C to 60 °C. A well-designed BTMS is a critical method to keep the cell temperatures within the desired range during charging and discharging [126,127]. During the normal EV or HEV operation, the battery modules are mostly over-heated due to their heat generation mechanisms except the case that it needs to be pre-heated to be charging or discharging healthily in an extremely cold environment [128]. To simplify the objective, this review focuses on the research about the effective air cooling methods for the BTMS, i.e., an effective air-cooling BTMS could dissipate excessive heat within the battery pack and control the maximum operation temperature below a certain value as well as maintain the maximum temperature differences within a required range. Air, liquid and PCMs are the three most common cooling media for the BTMS [29]. For liquid cooling BTMS, the heat is carried by the convection and conduction from the battery cells to the coolant via cooling channels. The coolant is usually water and Ethylene glycol solution, which could provide a wide operation temperature range from −40 °C to 105 °C. Due to the high thermal conductivity of these liquid coolant, the liquid cooling BTMS has both higher cooling capacity and cooling efficiency than other systems. To remove same amount of heat, the required flow rate for the liquid cooling BTMS is much lower than those for other systems due to the higher specific heat capacity values of the liquid coolant. In addition, the noise level of electric water pumps is usually lower than that of the same power electric air fans. On the other hand, the liquid cooling BTMS is usually large and heavy, compromising the overall driving range per charging of EVs and HEVs [129]. Due to the high electric conductivity of the water-based coolant, the sealing of the whole BTMS is critical to the safety of the system. The normal operating voltage of the electric motors in the EV is usually around 400 V, if the conductive coolant is leaked through the cooling channel into the electric motor, power module, or even the vehicle cabin, the consequences will be disastrous, such as short circuit, engine or power module failures, fire accidents, or even casualties to the driver, passengers, or maintenance technicians. To guarantee the absolute safety of using and maintaining high voltage electric vehicles, the sealing design is the priority of any liquid cooling BTMS design. As a result, the manufacturing cost of the liquid cooling BTMS is generally higher than that of the air-cooling BTMS. The main disadvantage of most solid-liquid PCMs is their relatively lower thermal conductivity, leading to excessive heat accumulations during normal or aggressive operations [130]. In extreme weather such as in hot summer or the desert region, the totally melt PCMs might become heat insulation materials adversely due to their low thermal conductivities [32]. On the other hand, the PCMs would need an extra amount of heating energy to warm the battery module before driving. The intrinsic thermal inertia of the PCMs makes them incapable of cooling down the battery modules at severe weather conditions. A comparison of the pros and cons of these three media is listed in Table 4 [131].

Compared with liquid and PCM cooling, the air-cooling BTMS has distinctive advantages including direct and safe access to the low viscosity coolant, small volume with simple structure and high compactness, lightweight, high design flexibility, low cost, low maintenance and high reliability [134]. The active cooling system such as liquid cooling consumes extra energy due to the additional water pump, shortening the total mileage of EVs or HEVs [135]. Park et al. [136] compared the numerical simulation results between air cooling and liquid cooling. Although the air cooling consumed an extra amount of power in a higher heat load condition, its basic advantages outweigh those of the liquid cooling in the low heat load conditions with a comparable amount of energy consumption. Giuliano et al. [137] focused on designing an air cooling thermal management system to sufficiently remove heat by using metal-foam based heat exchanger plates. They found the liquid cooling efficiency is not high enough due to the high electricity consumption of an HVAC (Heating, Ventilation, and Air-conditioning) unit

Table 4
Comparison of air, liquid and PCM cooling BTMS [131].

	Thermal conductivity	Structure complexity	Compactness	Weight	Uniform temperature distribution	Coolant viscosity	Cost	Maintenance
Air cooling [124]	M	L	H	L	L	L	L	L
Liquid cooling [132]	H	M	L	H	M	M	M	M
PCM based cooling [133]	L	H	L	H	H	H	H	H

*L - Low, M – Medium, H – High.

and coolant pump. Although many EV OEMs use liquid cooling as the primary cooling method for their EV battery packages, the air-cooling BTMS is still well adopted in large-scale commercial applications of low specific energy battery systems for EVs or HEVs with a stringent requirement of cost-down [138] as well as a loose requirement of fast charging and discharging operations [34]. Mass-volume commercial vehicles such as Honda Insight and Toyota Prius HEVs both adopted the air-cooling BTMS to manage their Lithium-ion battery modules with low manufacturing cost and high reliability [139].

3.1. Air-cooling BTMS applications

The advantage of air cooling is simple in structure without the requirement of cooling loops, easier to pack, low maintenance cost, no risk of liquid leaking into electronics or cabin, less weight and energy consumption. In the last couple of decades, a well-designed air-cooling BTMS was generally adequate for achieving desired performance in different climates for most parallel HEV applications [140]. Toyota Prius adopted the air-cooling BTMS for both 2010 Ni-MH battery packs and 2014 Lithium-ion battery packs to acquire the best cost performance. Volkswagen interestingly decided to substitute liquid cooling with air cooling on some battery packs of its hot-sale models [141]. One of its EV racing cars, being equipped with the air-cooling BTMS, won the Pikes Peak International Hill Climb in Colorado Springs in 2018 [142]. Lexus adopted the air-cooling BTMS for the 54.3 kW h lithium-ion battery pack in its first EV model UX300e [143]. Nissan successfully employed the active air cooling technology for its e-NV200 and leaf Lithium-ion pouch cell battery pack [144]. Roewe switched back to the air-cooling BTMS for its NCM523/LFP battery packs in its latest flagship model Marvel X. As the China cheapest EV, SAIC GM Wuling Hongguang Mini EV adopted the air cooling method for both its battery module and electric motor. Its sales volume in China had surpassed Tesla Model 3 in October 2020 with an astonishing number of 55,871 within three months since August 2020.

3.2. Conventional air-cooling BTMS designs

The air cooling method is widely used in the consumer electronics industry. The conventional air cooling solutions to electronic thermal management include [145]: heat sink with convective and radiative heat transfer structure, thermally conductive material development, heat pipes structure, an improvement, airflow optimization, and temperature monitoring etc … Since the beginning of the greenhouse gas emission trend and large-scale transport electrifications, the air cooling technologies were extended to the battery cooling applications in the EV and HEV industry. Fig. 1 shows a typical air-cooling BTMS. Fig. 1a is a

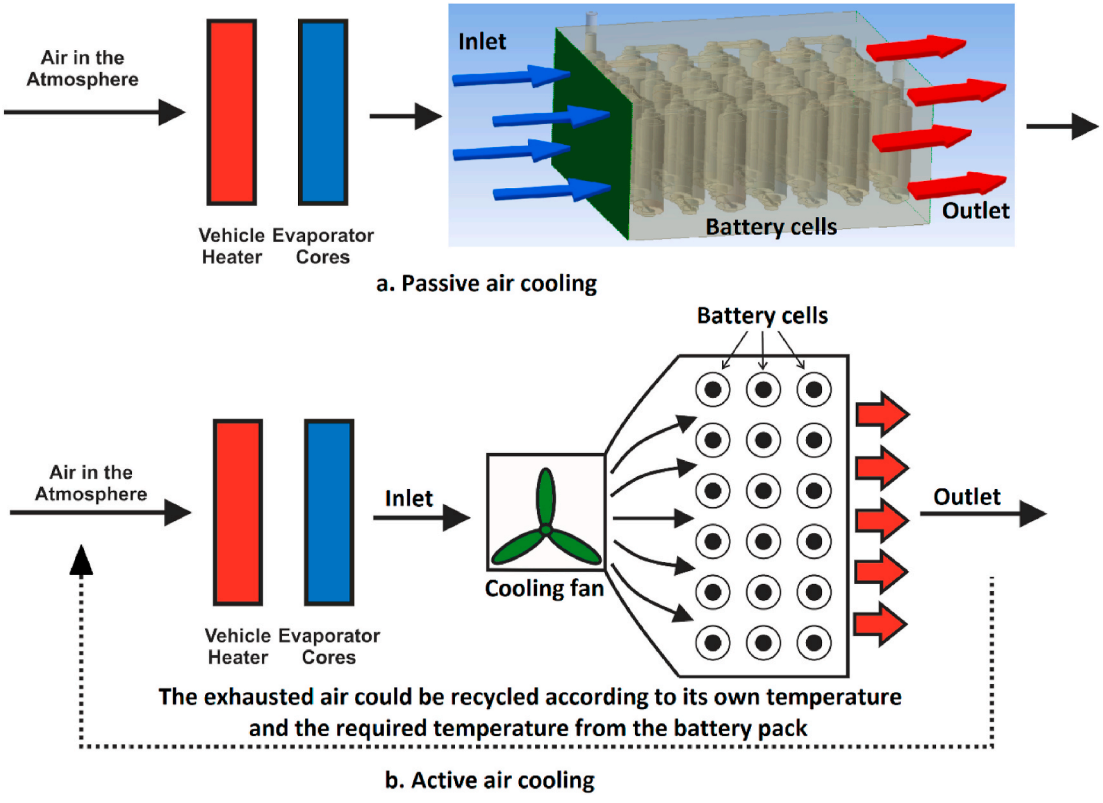

Fig. 1. A schematic diagram of the air-cooling BTMS.

typical Lithium-ion battery passive air-cooling BTMS in which battery cells are regularly aligned inside the battery pack. Outside air flows into inlets on one side of the battery pack by relative movement of the vehicle, passes through gaps between cells, and finally exits through outlets on the other side of the pack. The generated heat was carried away by air flow. Since the passive air cooling BTMS might not be sufficient when the car moves slowly or ambient temperature is relatively high, the active auxiliary method by adding fans or blowers to increase air flow rate is the necessary upgrade to ensure minimum cooling requirement. As shown in Fig. 1b, a basic active air-cooling BTMS consists of battery packs, cooling channels, inlets and outlets, as well as cooling fans [146]. Fans or blowers on either inlets or outlets could produce enough airflow to carry excessive heat or make temperature distribution more uniform. Although there are some disadvantages such as moderate cost increase, noise, and extra energy consumption, active air-cooling BTMS is still the mainstream cooling strategy for most OEMs due to its overall thermal and reliable performance. Park et al. [147] designed a conventional air-cooling BTMS for HEV to obtain a successful cooling performance. The single air cooling system made a good balance of fuel economy, cabin comfort, and manufacturing cost. Wang et al. [148] adopted a model to predict battery thermal behaviours during discharging both with and without air cooling. When the discharging rate is below the rate 3C and the ambient temperature is lower than 20 °C, active air cooling is not required. On the other hand, active air cooling may not be effective when the ambient temperature is above 35 °C, and much more fan power is required to keep the system temperature within an acceptable range.

3.3. Air-cooling BTMS design improvement

The air cooling solution affects the output, cost, and lifespan of battery packs directly and thus the vehicles' performance, manufacturing cost and service life, so all the parameters that influence battery pack should be optimized to achieve the top performance of the vehicles. The existing research work on improvement of the air-cooling BTMS can be classified into five categories: improvement on battery pack design, cooling channel improvement, inlet and outlet improvement, thermally conductive material improvement and secondary channel improvement, which are elaborated in the following sections.

3.3.1. Battery pack design improvement

Battery pack design can be improved by first optimizing the battery cell layout before the cooling channel improvement for the purpose of acquiring minimum battery pack volume and maximum specific energy. Erb et al. [149] proposed a cost function of battery cell sizes and BTMS costs. It was found that there was no universal cell size that could minimize the BTMS cost for every battery pack. The optimal cell size should be considered in the design phase for the specific battery pack to obtain optimal thermal performance with the lowest cost and maximum specific energy. However, as the EV and HEV industry is pursuing more reliable and standard products, battery cell sizes have been fixed to typical main models. Wang et al. [150] proved an axisymmetric battery pack layout that delivered the best cooling effect from different battery cell arrangements of 24 × 1 line, 8 × 3 rectangular, and 5 × 5 square layouts. The most effective fan location was the top of the cells pack. A 5 × 5 pack was the favourite battery pack layout in terms of the cooling performance and cost reduction. Kang et al. [151] arranged battery cells into different arrangements to acquire optimal cooling effects. It was reported that the rectangular arrangement was better than the square one due to its lower maximum temperature pattern without the active cooling. They also found that in the air-cooling BTMS, the heat transfer was mostly achieved by thermal conduction than thermal convection if the coolant inside the BTMS satisfied the Rayleigh number. Similar research was conducted by Zhang et al. [152] to improve battery thermal safety by exploring various cell arrangements and distances. The ring-shaped arrangement exhibited the worst thermal performance with the maximum temperature, maximum temperature difference and deviation. On the other hand, the line-shape arrangement showed better thermal performance at the 1C, 2C and 3C discharging rate. To meet the cooling requirements, the cell-to-cell distance was recommended to be at least 7 mm.

The performances of two different arrangements of LFP cylindrical cells (aligned and staggered arrangements) was compared and analysed in a key national laboratory at the Xi'an Jiaotong University [153]. The temperature rise was affected by the longitudinal distance in the staggered battery cell arrangement. The maximum temperature difference could be reduced by enlarging the transverse distance at the cost of maximum temperature rise. After balancing the different design requirements using simulation results, the aligned arrangement with a longitudinal distance of 34 mm and a transverse distance of 32 mm was the optimal solution. Fan et al. [154] compared three cell arrangements: aligned, staggered and cross. The aligned one exhibited the highest cooling effectiveness as well as the lowest power consumption. The cooling capacity increased with the growing air inlet velocity. However, there was a threshold of the improvement of the cooling performance because the power consumption rose exponentially as the air inlet velocity increased. Ye et al. [155] developed a new air cooling model by tilting the battery pack case with a 5° angle. The tilting air flow channel decreased air flow resistance. The simulation results revealed that the maximum temperature was largely reduced, and the heat dissipation performance was improved. Chen et al. [156] focused their study on the parallel cell arrangement and cell distances. The author combined the network flow resistance model and the heat transfer model to investigate the cooling performance of the air-cooling BTMS. The simulations exhibited a reduction of 42% in maximum temperature difference using the parallel cell arrangement. A longitudinal axial cell arrangement was extensively investigated by Yang et al. [157]. The axial air flow channels formed by the cell layout could carry away more heat than the conventionally designed channels. The larger radial distance between the cells could lead to lower power consumption at the cost of space efficiency reduction by about 30%. Yu et al. [158] developed a three-stack battery pack with the stagger-arranged Lithium-ion battery cells on each stack with two options: natural air cooling and forced air cooling as shown in Fig. 2. The experimental results showed that the active air cooling method could reduce the maximum temperature significantly.

Severino et al. [159] developed a novel Multi-Objective Evolutionary Algorithm approach to achieving the optimal battery pack design by obtaining broad possible solutions of different parameters including cell number, cell distance, and inlet channel positions. Li et al. [160] shrank battery pack volume to save more space for cabins. A multi-objective optimization model was built to obtain an ideal battery pack design with the combination of small pack volume, low-temperature difference, as well as low-temperature standard deviation. The simulation results showed a volume reduction of 34.2%, a reduction of 51.9% in the maximum temperature difference, and a temperature standard deviation curtailment of 70.0%.

3.3.2. Cooling channel improvement

Once the battery pack arrangement is selected, the cooling channel design is the next objective of the optimization works. Fan et al. [161] designed a battery pack with an unevenly-spaced channel on both cell surfaces. They conducted three-dimensional transient thermal analyses of the modified modules and concluded that the two-side cooling with a moderate widening of the unevenly distributed channels improved the temperature uniformity more effectively. Xun et al. [162] found that enlarging channel diameter could improve the cooling effect but would result in more uneven temperature distribution. According to the simulation results, the inlet air Reynolds number was suggested to be around 2000 or higher at the 2C discharging rate. In another study [163], the heat dissipation was improved by substituting the longitudinal battery pack with the horizontal one. A novel design called

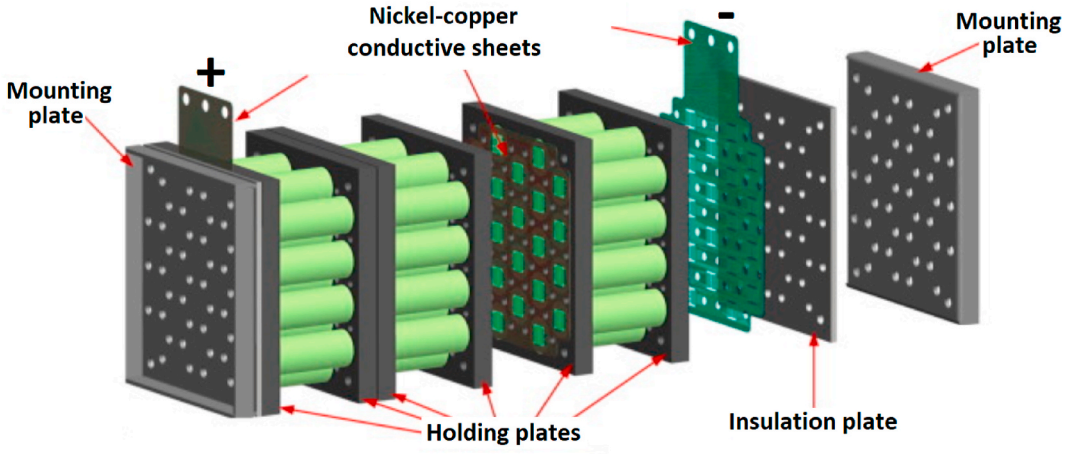

Fig. 2. Three-stack battery pack with stagger-arranged Lithium-ion battery cells on each stack (Ref. [158]).

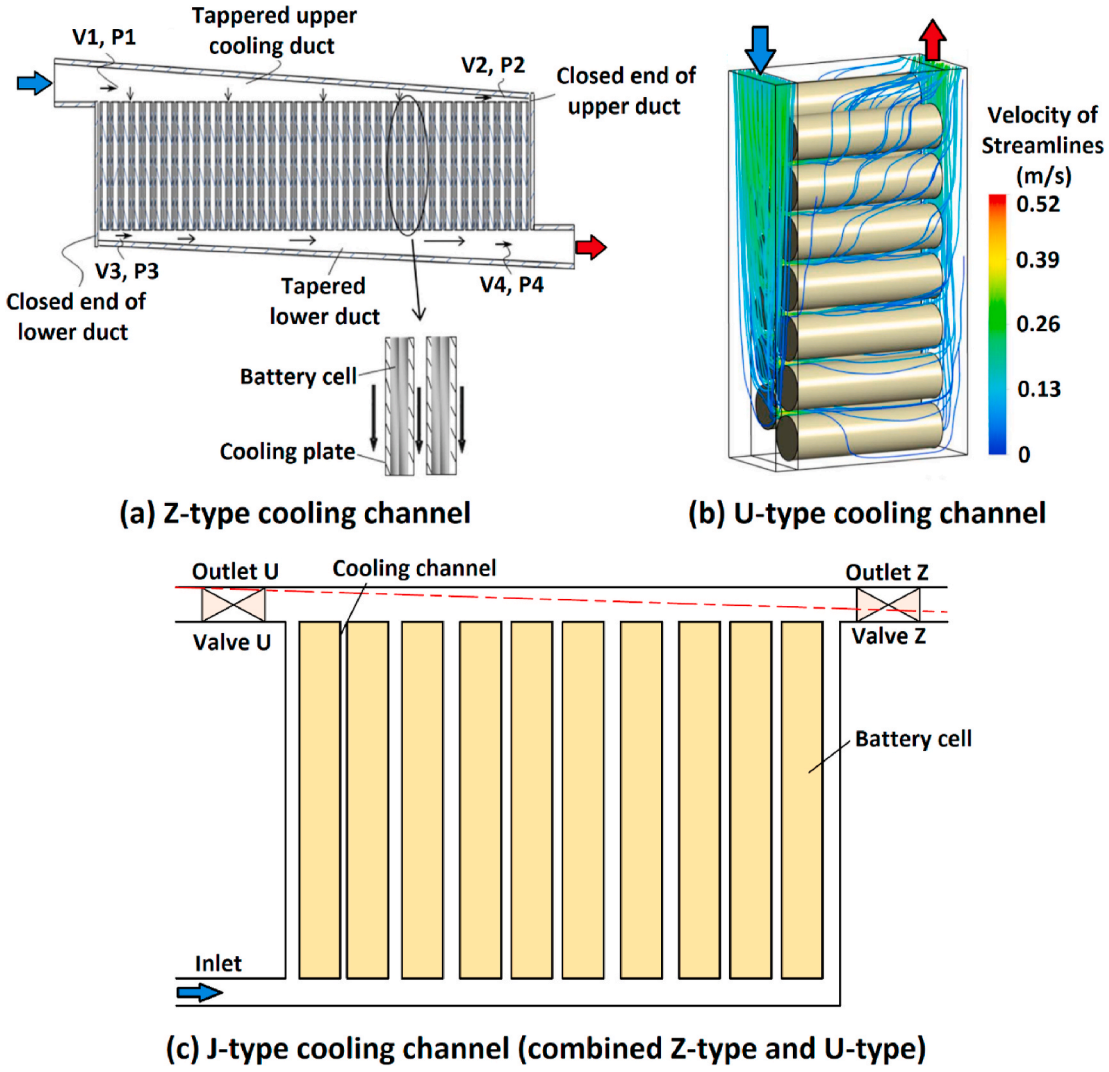

Fig. 3. Different cooling channel designs.

"bottom double U duct mode" demonstrated more uniform temperature distribution and less temperature rise. Since 90% of SOC was an upper threshold for the maximum temperature rise and difference, it should be avoided if the active air cooling capacity could not meet the requirement. Both charging and discharging rates were recommended to be controlled below certain values to guarantee effective cooling performance. In another study, a "Z-type" air flow channel with the tapered inlet and outlet was designed by Sun et al. [164] to improve the cooling performance (Fig. 3a). The tapered ducts were proven to be able to relieve the fluctuation of the air flow rate, reduce the temperature variation, and decrease the total airstream pressure drop. The additional orifice structure could channel the air flow from the major duct to the minor duct within the cooling channels to reduce the maximum temperature by about 1.1 °C. The aluminium corrugations were inserted appropriately with suitable length, thickness, and contact pressure between the cooling plates to expand the heat transfer areas to enhance the cooling efficiency to about 93% and reduce the maximum cell temperature by about 0.4%. Substituting the aluminium cooling plate with the copper one and thickening the aluminium cooling plate could reduce the maximum temperature by 0.3 °C and 0.6 °C, respectively. Chen et al. [165] optimized the "Z-type" cooling channel design by choosing the favourable plenum angles and widths. A flow resistance network model with computational fluid dynamics (CFD) verification was conceived to obtain accurate flow rates of the cooling air. Different plenum angles, divergence widths and convergence widths were simulated using a Newton method via nested loop procedure to find the optimal combination. Although different divergence and convergence plenum angles did not deliver obvious efficiency improvement, suitable plenum widths were proven to be able to reduce the temperature nonuniformity. Lu et al. [166] designed a "U-type" (Fig. 3b) cooling channel BTMS with a top inlet and outlet to acquire a better cooling performance. Its maximum temperature difference was 3 K lower than the corresponding "Z-type" design. Additionally, Liu et al. [167] proposed an innovative "J-type" cooling channel BTMS by combining "U-type" and "Z-type" designs strategically (Fig. 3c). The novel BTMS real-time control system controlled the two outlet valves by switching channel configurations between "U-type" and "Z-type" according to the feedback of the thermal condition of the battery pack. An optimal control strategy was developed to improve system temperature uniformity.

Yu et al. [168] proposed a two-directional cooling channels design to accelerate heat dissipation and uniformize the heat distribution inside the battery pack. Two independent cooling channels and two fans were used to improve the cooling effect. The extra cooling fan contributed to the additional electricity consumption other than vehicle motor and inverter modules. As a result, the total range of the vehicle was compromised. Fathabadi [169] used the distributed thin air flow ducts to obtain better cooling efficiency. This design outperformed other designs until the ambient temperature reached 48 °C in terms of the maximum temperature, temperature uniformity and voltage distributions in a natural convection scenario. Even when the ambient temperature was as high as 48 °C–55 °C, the desired temperature range could still be achieved with the help of a suitable electric fan above the battery module. The optimized air-cooling BTMS design also exhibited a smaller battery pack volume increment. Zhou et al. [170] conceived novel airflow ducts with the distribution orifices longitudinally aligned along with it as sub-flow channels. The evenly aligned orifices along the airflow ducts distributed the inlet cold air into different parts of battery cells, blowing away heat through distances between cells towards four edges of the battery pack. Increasing the size (1.5 mm) and quantity (5 rows) of the orifices was proven to be useful to acquire a lower maximum temperature (from 325.9 K to 305.7 K) and more uniform temperature distribution (maximum temperature difference $\leq$ 3 K). Lu et al. [171] designed two kinds of thin airflow ducts within the battery pack: 15 ducts and 59 ducts. The simulation results showed that a 59-ducts channel design was recommended due to its higher heat transfer efficiency between the airflow channels and the battery cell surfaces compared with the 15-ducts channel design, with decreases of maximum temperature from 316 K to 310 K and maximum temperature difference from 22 K to 16 K. Another conclusion was that the maximum temperature would be decreased by enlarging the sizes of cooling channels.

The reciprocating airflow is another cooling channel improvement method without literally improving the air flow channels. Wang et al. [172] developed an actively controlled reciprocating cooling strategy to reduce both the power consumption and overall temperature non-uniformity. The experimental results showed that the reciprocating cooling was able to decrease the maximum temperature by up to 15%. The cooling flow consumption from the reciprocating control strategy could also be saved by up to 50% with an insignificant increment of the maximum temperature. The active reciprocating cooling could also greatly improve the temperature uniformity than the one direction cooling method. Na et al. [173] proposed a two-directional double-layer design with two adjacent channels separated by a diathermanous board aiming to enhancing heat conduction and improving temperature uniformity. Compared with the unidirectional channel design, this two-directional double-layer air flow design delivered a lower maximum average temperature difference by 1.1 K (47.6% reduction). Soltani et al. [174] developed a 3D-thermal Lithium-ion battery pack model to obtain an optimal cooling performance by arranging and combining three parameters: battery distance, air velocity and fan position. The optimal simulation result was a 5 mm inter-cell distance with two fans on one side blowing the air flow at a velocity of 5 m/s. This optimization was also validated using solid experimental data with a temperature error of less than 2 °C.

3.3.3. Inlet and outlet improvement

Some researchers focused on improving the inlet and outlet designs to improve the cooling effect. The heat dissipation capacity might have a non-linear relationship with the entrance size [175], but the inlet/outlet's position and shape had prevailing effects on the overall cooling performances. Chen et al. [176] compared the inlet/outlet positions of different air-cooling BTMSs. After CFD simulations, the optimal inlet and outlet positions were both in the middle of the width side of the prismatic cells battery pack. The maximum temperature was decreased by 4.3 K compared with the original "Z-type" channel design while the maximum temperature difference was decreased by 6.0 K. The CFD simulation methodology could obtain the optimal solution with just several pieces of calculations regardless of the BTMS design and operating parameters. Chen et al. [177] modified a conventional air-cooling BTMS to an asymmetrical structure with an unequal cell-spacing distribution to obtain the optimal cooling performance. They made three conclusions: i) the temperature uniformity, as well as the maximum temperature, were inversely related to the number of battery cells; ii) the cooling performance of the symmetrical structure was better than that of the asymmetrical one; iii) an optimal uneven cell-spacing distribution design might deliver the best cooling performance. Wang et al. [178] proposed an active air-cooling BTMS to protect the battery pack from excessive heat accumulation during normal discharging. The overall cooling performance of Design 1, including both the maximum temperature difference and maximum temperature, was better than that of Design 2 as shown in Fig. 4.

E et al. [179] simulated three inlet/outlet positions to acquire an optimal solution: up inlet and down outlet, same-side inlet and outlet, and different-side inlet and outlet. The results showed that placing the inlet and outlet on opposite sides of the battery pack was the optimal solution. An additional baffle structure was utilized to prevent the air flow from passing through the surrounding distances between the case and cells instead of flowing through the inter-cell distances. Shahid et al. [180] added an inlet plenum to change the air flow direction. This simple modification significantly decreased the air recirculation and eliminated the dead-air regions inside the package. The optimal nozzle length and Reynolds number were obtained from the simulations to

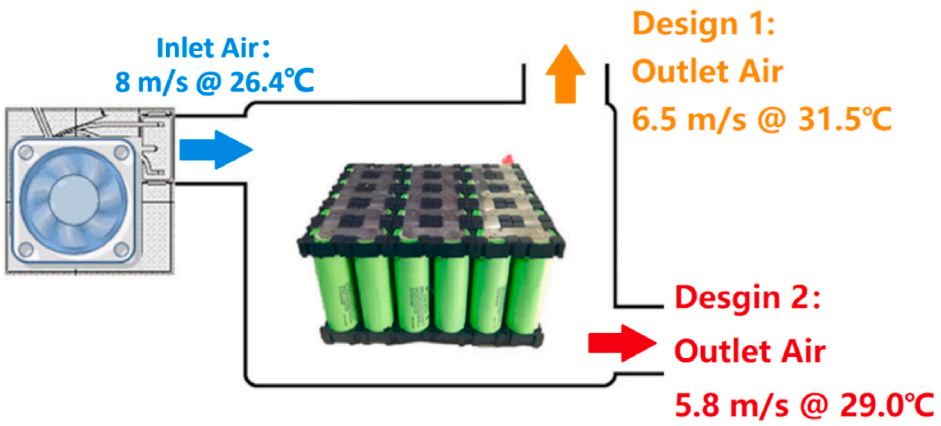

Fig. 4. BTMS designs with different outlets: Design 1: upper outlet; Design 2: bottom outlet (Ref. [178]).

achieve a reduction of maximum temperature and maximum temperature difference by 18.3% and 54.6%, respectively. Shahid et al. [181] incorporated an inlet plenum, jet inlets, and multiple vortex generators into an air-cooling BTMS. The maximum temperature and maximum temperature difference were decreased by about 5% and 21.5%, compared with the original configuration. The temperature uniformity of a single cell was also reduced from 4.94 °C to 4.13 °C. The cooling requirement was achieved with almost no mass flow increment or more power consumption. Chen et al. [182] explored the cooling performance of the air-cooling BTMS with different discharge rates, air flow rates, inlet & outlet plenum angles and cell spacings. The low inlet air design could barely decrease the maximum temperature and maximum temperature difference. The high air flow rate and small cell spacing would cause higher electricity consumption. By optimizing the inlet and outlet plenum angles, the air-cooling BTMS thermal performance was improved significantly without expanding the pack volumes or increasing the electricity consumption. Heesung [103] improved the cooling performance and saved the cost by applying the tapered manifold and adding the pressure relief ventilation holes instead of modifying the whole air-cooling BTMS structure. Simulation results indicated that the maximum temperature was effectively controlled by this novel design. But the overall power consumption of the cooling fan was also increased due to the extra ventilation holes.

Based on the "Z-type" cooling channel design, Hong et al. [183] proposed a secondary ventilation outlet hole design to reduce the maximum temperature difference. The locations of the secondary ventilations were suggested to be on the battery pack case surfaces opposite to the cooling channels with the highest temperature. Zhu et al. [184] proposed a theoretical model to simulate the battery heat generation and dissipation. The relationship between the SOC and the reversible heat generation rate was much stronger than that between the SOC and the irreversible heat generation rate. A cooling fan on the outlet was added to create a negative pressure environment inside the battery pack compared with the conventional cooling fan position on the inlet. The battery pack resistance coefficient was recommended to be higher to obtain a more compact battery pack.

3.3.4. *Thermally conductive material improvement*

Due to the space limitations under the cabin or somewhere else inside the vehicle frame, there is usually not enough volume margin for modifying or redesigning the general structure of the battery pack. As a result, other methods with no volume or layout change should be considered. A special kind of aluminium foam was proposed by Saw et al. [185] to enhance cooling performance. The smaller foam porosity not only reduced the surface temperature but also increased the friction factor of the cooling channels. The fibres inside the foam would produce more turbulent flows to enhance heat transfer between the cooling channel and air.

Li et al. [186] invented a novel thermal conduction structure combining a double silica cooling structure with the copper meshes as shown in Fig. 5. The excellent heat dissipation performance and prominent temperature uniformity during a high discharging rate were observed from the simulation results. It demonstrated good potentials to be applied in the pouch battery and prismatic battery applications.

Mohammadian et al. [187,188] embedded porous aluminium foams into an air cooling aluminium pin-fin heat sink. A 70% cooling channel inner surface coverage with both aluminium pin fins and porous aluminium foam insertions was recommended to achieve the optimal

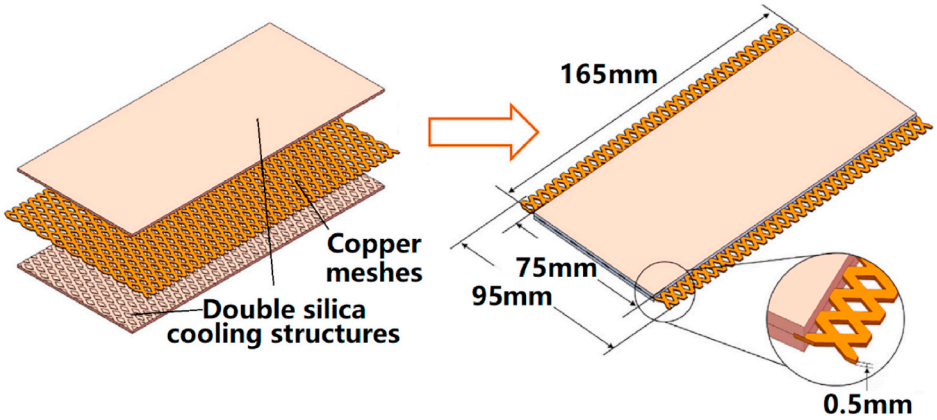

Fig. 5. Double silica cooling structure with copper meshes (Ref. [186]).

temperature uniformity as well as reduce the maximum temperature. Kizilel et al. [133] introduced PCMs into an air-cooling BTMS to set up a passive thermal management subsystem to alleviate the rapid heat accumulation under extreme conditions such as over 45 °C ambient temperature or over 2C charging or discharging rate. The results showed that the novel subsystem operated safely during the high *C*-rate discharging. Jilte et al. [189] combined an active air cooling method with a passive PCM cooling method. Each cell was surrounded by a 4 mm thick layer of PCMs interconnecting with each other. The air cooling channels were evenly orientated within the straight-line battery pack to improve the temperature uniformity (cell temperature uniformity less than 0.05 °C during 2C discharging and 0.12 °C during 4C discharging). In another research conducted by Qin et al. [190], PCMs were adopted to support active air cooling. Both the maximum temperature and maximum temperature difference were kept below the requirement during the 1–4C rate discharging. The active cooling model was proven to have better thermal performance than the passive ones. Mehrabi-Kermani et al. [191] embedded paraffin as PCMs in a copper foam. The high thermal conductivity of the copper foam (effective thermal conductivity reached 11.98 W m^{-1} K^{-1}) resulted in uniform temperature distributions over a longer period of normal working cycles (33 min below 60 °C instead of 5–9 min by other cooling methods).

Luo et al. [192] combined an active air cooling design with a silica cooling plate-aluminate thermal plate structure to achieve a better cooling effect and small temperature difference for a pouch cell module. The results showed that the novel cooling plate decreased the maximum temperature during a high *C*-rate discharging compared with the basic natural convection and single silica cooling plate designs. Saw et al. [193] designed a mist air-cooling BTMS as the "version 2.0" of the conventional dry air cooling system. Water mist was used as an additive to increase the specific heat capacity of the dry air. This new version could provide a more uniform temperature distribution. A 3% mist fraction with 5 g/s flow rate was proven to be adequate to keep the cell surface temperature below 40 °C. Showing the advantages of the simple structure and lightweight, the mist air-cooling BTMS is regarded as an encouraging economic replacement to the liquid cooling BTMS. Sefidan et al. [194] injected a water and Al_2O_3 nanofluid as an auxiliary thermally conductive material into an aluminium cylindrical tank surrounding the battery cells. The cooling efficiency and temperature uniformity of this novel heat transfer cylinder were proven to be higher than those of the conventional air-cooling BTMS (16–24 K reductions for high-risk cell maximum temperatures). Zhao et al. [195] integrated a direct evaporative cooling (DEC) design into the air-cooling BTMS to decrease the inlet air temperature. The cooling performance of the DEC model was better than that of the natural convection and forced air cooling models. The DEC method was able to cope with higher ambient temperature operations with lower cooling fan power consumptions, which was beneficial to the applications of adverse weather and high energy consumption conditions such as EVs and HEVs.

3.3.5. Secondary channel improvement

Some researchers proposed secondary channel designs to optimize system. A pin-fin heat sink design [196] was carried out to decrease the maximum temperature and temperature deviation. Three-dimensional

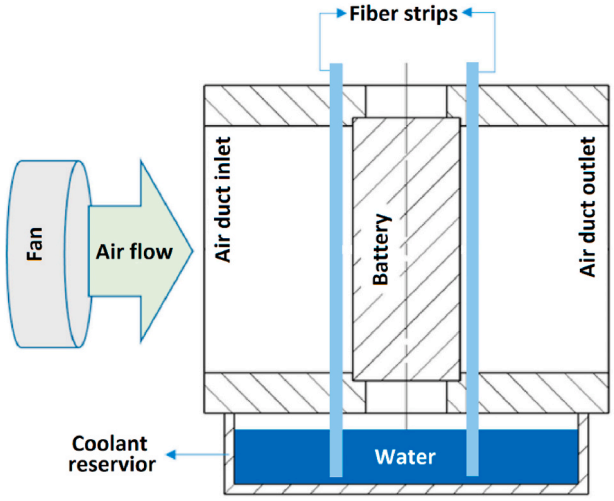

Fig. 7. A basic air cooling duct with secondary hydrophilic fibre channels (Ref. [200]).

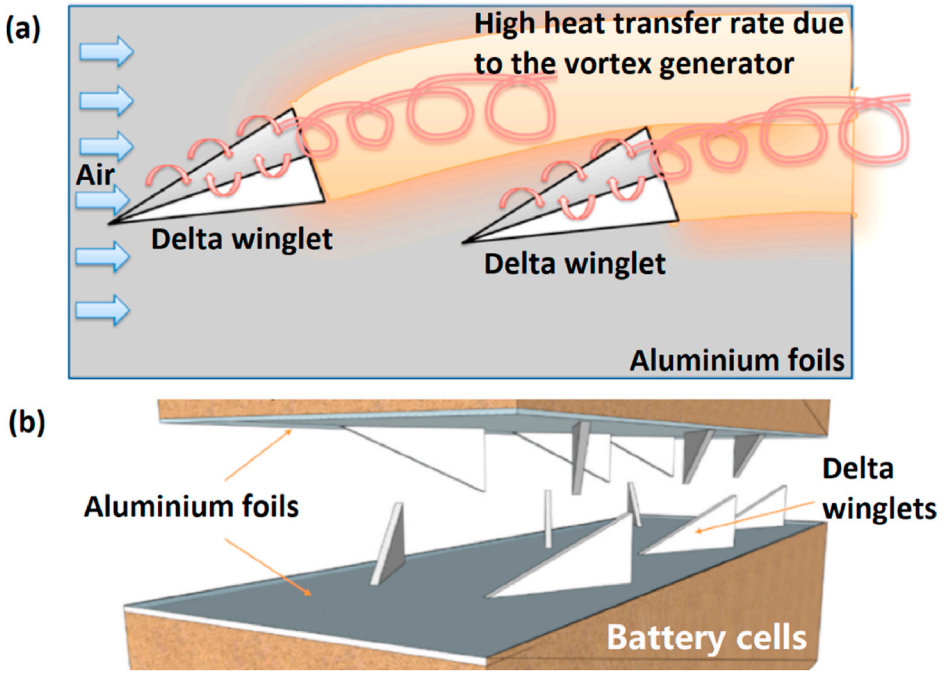

Fig. 6. Delta winglets design: (a) vortex generator; (b) winglets arrays (Ref. [198]).

simulation results showed that its cooling effect was better than the conventional BTMS without any secondary channel structures. Dan et al. [197] designed a micro heat pipe array (MHPA) as a secondary channel. Simulation results showed that the MHPAs inside the cooling channels provided a timely response to the transient-shifting or unstable operating scenarios. Lower temperature rise and fluctuation were observed in the air-cooling BTMS with MHPA structures than those without any secondary channel improvement designs. Han et al. [198] installed several arrays of the tightly packed delta winglets inside the cooling as shown in Fig. 6. These small secondary winglets generated local air vortexes and achieved a heat transfer rate of 150–200 W/K. This novel secondary channel structure could be a viable solution for air-cooling BTMSs. Li et al. [199] proposed an air-cooling BTMS with novel herringbone fins design in staggered cells configuration. The optimal design with herringbone fins in a staggered arrangement could decrease the average temperature by 4.15 K at an inlet air velocity of 0.15 m/s during the 3C rate discharging. An evident temperature uniformity improvement was observed both within and among the battery cells when the herringbone fins structure was adopted to the basic air-cooling BTMS.

Wei et al. [200] added secondary hydrophilic fibre strips structure to a basic air cooling duct to increase its cooling efficiency in Fig. 7. The coolant in the bottom reservoir was driven by the capillary forces to climb along the microfibre channels, which could absorb the heat from the battery cells by the water evaporation effects. In the experimental study, the temperature uniformity was improved by 56% compared with the basic air-cooling BTMS design.

3.3.6. Cell cooling strategies

Except for the cooling strategies on the whole battery system level, there are other cooling methods aiming at specific hotspots of the battery cells such as electrode tabs and welding points. Zhao et al. [201] found that the thermal resistance between electrodes and current collectors was too high to be ignored due to the high ohmic resistance of the welding connections. As a result, the tab cooling method is specially designed to be compared with the traditional surface cooling method in Fig. 8. The experimental results showed that the surface cooling method exhibited more uneven temperature distributions within the battery active regions, causing severer capacity fading, while the tab cooling method delivered more uniform current and temperature performances at high charging and discharging rates, extracting more capacity. Hunt et al. [202] concluded that tab cooling could prolong about 200% lifetime of the EV Lithium-ion batteries. On the other hand, Dondelewski et al. [203] suggested the optimal selection between surface cooling and tab cooling methods should be based on the required lifetime and the trade-offs between potential capacity fading and output performances. Li et al. [204] investigated the cooling performances of different tab and cell configuration designs and found that multiple tabs cooling delivered minimum temperature inhomogeneity due to the more uniform internal current densities as well as moderate heat generation rates. Heimes et al. [205] proposed a novel liquid tab cooling design for Lithium-ion pouch cell batteries to cool down the contact area more efficiently between tabs and current collectors. The simulation results exhibited that it was a feasible solution to cool down the battery cells during 1C fast charging and delivered dynamic power performances. Patil et al. [206] combined the tab cooling with the dielectric fluid immersion cooling to enhance the BTMS cooling performance. During 3C discharging, the novel hybrid design exhibited 46.8% lower maximum temperature at the positive tab than the natural convection design. Both the simulation and experimental results showed that the combination of two cooling methods would be a promising candidate for the high energy density and capacity Lithium-ion battery pack applications on the future EVs and HEVs.

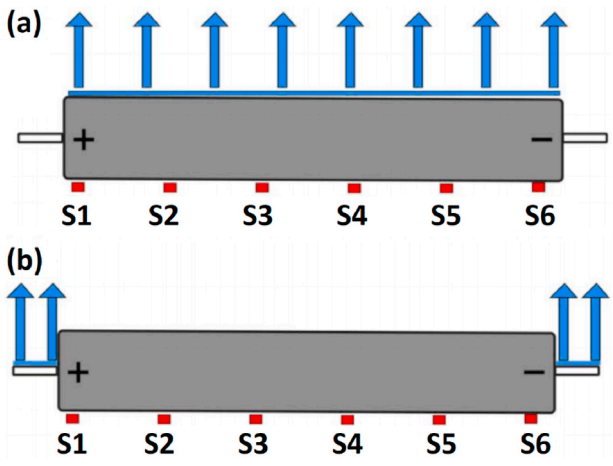

Fig. 8. Two cell component cooling methods: (a) surface cooling method; (b) tab cooling method (Ref. [201]).

4. Discussions

The life cycle cost of the EVs and HEVs mostly comes from the battery system in terms of the power output and service life [207]. The Lithium-ion battery's working performance and service life are significantly determined by the operating temperature and ambient temperature. The mismanagement of the crucial temperature pattern of any battery packs, including both the temperature range and uniformity, will adversely lead to a shortened battery lifetime, fading capacity, and, in some extreme cases, safety hazard such as thermal runaway and explosion [33]. In addition to the battery temperature management system performance, the manufacturing cost is also one of the key elements to the success of the EV and HEV original equipment manufacturers (OEMs). The cost performance of any automobile model has a dominant influence on the final sales volume [208]. The prices of EVs were usually twice those of the comparable petrol-fuel engine vehicles. Almost half of the EV manufacturing cost came from the battery system [209]. After fulfilling the basic requirement from the designers and customers, cost reduction projects played a critical role in helping OEMs make more profits by large-volume productions [210]. Compared with other cooling methods, the air-cooling BTMS has the lowest manufacturing cost with the most compact and reliable structure. This is simply the reason why the air-cooling BTMS has never gone out of any OEMs' sights for EV and HEV applications.

Most electrolytes of the Lithium-ion batteries are liquid-based, which means their high-temperature tolerance is not as high as that of solid-based electrolyte batteries mainly due to the lower boiling point limit of the liquid-based electrolytes. One of the favourite features of the all-solid-state battery is its wide operating temperature range, especially at high temperatures. In other words, if a well-designed air-cooling BTMS can handle with liquid-based electrolyte Lithium-ion batteries, it will be more competent for the all-solid-state Lithium-ion battery systems in the future. Kisu et al. [211] studied the mechanical stability and electrochemical stability of the $LiBH_4$-based solid electrolytes. The experimental results provided useful complex hydride solid electrolytes for all-solid-state Lithium-ion batteries with Lithium metal anodes. Zhang et al. [212] developed a Poly Ethylene Oxide (PEO-based) solid polymer electrolyte for an all-solid-state Lithium battery by changing the PEO amorphous domain via a simplified UV-derived reaction. The improved solid polymer electrolyte exhibited both higher ionic conductivity and mechanical stability, delivering better cycling performances with the fewest Lithium dendrite structures. Zhang et al. [213] developed a ceramic-based solid $Li_{6.75}La_3Zr_{1.75}Ta_{0.25}O_{12}$ electrolyte by a solution casting method as well as a $LiNi_{0.5}Co_{0.2}Mn_{0.3}O_2$ cathode to produce an advanced solid-state Lithium-ion battery with high ionic conductivity, high Lithium-ion transference efficiency, wide electrochemical range, and stable thermal performances. The cycling experimental results showed the great potential of the high-energy-density solid-state

Lithium-ion batteries to be applied in the EV industry. Nguyen et al. [214] investigated a one-step scalable Na_3PS_4 solid electrolyte synthesis method. The novel method could reach high ionic conductivity within 20 min, which was better than many other multiple-step methods. The all-solid-state battery with this Na_3PS_4 solid electrolyte delivered a capacity of 185 mA h/g during the first discharging process. If the all-solid-state battery technology is well-developed in the next decade, the cost-saving and highly reliable active or passive air-cooling BTMS will be good enough for the EVs and HEVs.

There is probably no existing BTMS that could meet all requirements such as excellent safety performance with a low manufacturing cost, superb power output accompanied by negligible battery capacity degradation, supreme cooling efficiency with slight power consumption, high structural compactness with exceptional thermal transfer capacity, as well as remarkable airflow intensity with low noise ergonomic experience etc. According to the cyclical model of technological changes, after cyclic processes of diversified concepts, continuity, novelty and selection, the specific artifacts will be finally replicated. For example, the evolution of bicycles finally converged to the standard design of two wheels, rear chain, and air tires from more than ten different forms. In the end, the evolution of the air-cooling BTMS in HEVs and EVs will inevitably reach optimal designs after miscellaneous technical variations, industrial standard selections, and retentions. The odds of the air cooling method being an optimal choice for the BTMS in HEVs and EVs after numerous optimizations are possibly high. Akinlabi et al. [36] concluded that air flow channel optimization is the most effective method so far. This paper would likely to put the eggs into different baskets: battery layout, inlets & outlet designs, as well as secondary channel structures designs, are all beneficial to the overall improvements of the BTMS cooling performances. Furthermore, with the promising development of all-solid-state battery technology and advanced battery materials with better thermal durability [208], the power battery is becoming more thermally stable with wide temperature durability, and thus the air-cooling BTMS is promising to play a major role in the future BTMSs for EVs and HEVs.

5. Conclusions

This paper reviewed the air-cooling BTMS technology and the recent improvement designs used in EVs and HEVs. The improvement of the cooling channel designs was found to be the most popular optimization method for improving the performance of the air-cooling BTMS. The substructure improvements such as inlet, outlet, and secondary channel could further enhance the cooling effect. The applications of novel substructures, such as fins and winglets, would increase the local turbulence and enhance the convective heat transfer within the channels to minimize the hotspots. Furthermore, the combination of state-of-the-art thermally conductive materials, as well as the cooling technologies such as heat pipe and direct evaporative cooling, would further raise the cooling capability of the air-cooling BTMS. Nonetheless, there are still some extreme conditions under which the single air-cooling BTMS is not capable of dealing with such as long-time high charging or discharging *C*-rate operations, extremely high ambient temperatures and unpredicted battery malfunctions or thermal runaways. To make up the air cooling capacity, design innovations on new substructures and even conjugated cooling systems combining PCM structures with the air cooling technique can be developed. Novel inlet air pre-processing methods, including liquid cooling, HVAC system, thermoelectric coolers, or DEC etc., can be figured out to cool down the battery cells under hot weather conditions. With these advanced enhancement techniques, the air-cooling BTMS is promising to provide adequate cooling for even higher energy density battery systems used in EVs and HEVs.

Declaration of competing interest

The authors declare that they have no known competing financial interests or personal relationships that could have appeared to influence the work reported in this paper.

Acknowledgment

The authors gratefully acknowledge the financial support provided by the Australian Research Council (LP170100879).

References

[1] L.H. Martinez, Post industrial revolution human activity and climate change: why the United States must implement mandatory limits on industrial greenhouse gas emmissions, J. Land Use Environ. Law (2005) 403–421.
[2] O. Edenhofer, Climate Change 2014: Mitigation of Climate Change, Cambridge University Press, 2015.
[3] IEA. CO2 emissions by sector. https://www.iea.org/data-and-statistics?country=WORLD&fuel=CO2%20emissions&indicator=CO2BySector (accessed 3 December, 2020).
[4] W. Yuan, H.C. Frey, T. Wei, N. Rastogi, S. VanderGriend, D. Miller, L. Mattison, Comparison of real-world vehicle fuel use and tailpipe emissions for gasoline-ethanol fuel blends, Fuel 249 (2019) 352–364.
[5] X. Sun, Z. Li, X. Wang, C. Li, Technology development of electric vehicles: a review, Energies 13 (1) (2020) 90.
[6] O. Gippner, D. Torney, Shifting policy priorities in EU-China energy relations: implications for Chinese energy investments in Europe, Energy Pol. 101 (2017) 649–658.
[7] M. Debert, G. Colin, G. Bloch, Y. Chamaillard, An observer looks at the cell temperature in automotive battery packs, Contr. Eng. Pract. 21 (8) (2013) 1035–1042.
[8] P. Wolfram, N. Lutsey, Electric Vehicles: Literature Review of Technology Costs and Carbon Emissions, The International Council on Clean Transportation, Washington, DC, USA, 2016, pp. 1–23.
[9] G. Berckmans, M. Messagie, J. Smekens, N. Omar, L. Vanhaverbeke, J. Van Mierlo, Cost projection of state of the art lithium-ion batteries for electric vehicles up to 2030, Energies 10 (9) (2017) 1314.
[10] F.V. Conte, Battery and battery management for hybrid electric vehicles: a review, E I Elektrotechnik Inf. 123 (10) (2006) 424–431.
[11] Z.M. Salameh, M.A. Casacca, W.A. Lynch, A mathematical model for lead-acid batteries, IEEE Trans. Energy Convers. 7 (1) (1992) 93–98.
[12] S. Ovshinsky, M. Fetcenko, J. Ross, A nickel metal hydride battery for electric vehicles, Science 260 (5105) (1993) 176–181.
[13] S. Yoon, J. Lee, T. Hyeon, S.M. Oh, Electric double-layer capacitor performance of a new mesoporous carbon, J. Electrochem. Soc. 147 (7) (2000) 2507–2512.
[14] L.H. Saw, Y. Ye, A.A.O. Tay, Integration issues of lithium-ion battery into electric vehicles battery pack, J. Clean. Prod. 113 (2016) 1032–1045.
[15] L.I.R. Batteries, Technical Handbook, disponible 25, 2013, pp. 27–29, http://cardi.igeofcu.unam.mx/techdocs/PowerSonic_batteries.pdf.
[16] M.S. Whittingham, Materials challenges facing electrical energy storage, MRS Bull. 33 (4) (2008) 411–419.
[17] G. Pistoia, Lithium-ion Batteries: Advances and Applications, Newnes, 2013.
[18] N. Nitta, F. Wu, J.T. Lee, G. Yushin, Li-ion battery materials: present and future, Mater. Today 18 (5) (2015) 252–264.
[19] A. Mahmoudzadeh Andwari, A. Pesiridis, S. Rajoo, R. Martinez-Botas, V. Esfahanian, A review of Battery Electric Vehicle technology and readiness levels, Renew. Sustain. Energy Rev. 78 (2017) 414–430.
[20] N. Sato, Thermal behavior analysis of lithium-ion batteries for electric and hybrid vehicles, J. Power Sources 99 (1–2) (2001) 70–77.
[21] S. Al-Hallaj, J.R. Selman, Thermal modeling of secondary lithium batteries for electric vehicle/hybrid electric vehicle applications, J. Power Sources 110 (2) (2002) 341–348.
[22] L. Fred. Tesla Model 3: exclusive first look at Tesla's new battery pack architecture. Electrek. https://electrek.co/2017/08/24/tesla-model-3-exclusive-battery-pack-architecture/(accessed 31 December, 2019).
[23] C. Luca. BMW plans different sized battery cells to preserve design of future models. Automotive News Europe. https://europe.autonews.com/article/20180418/ANE/180419811/bmw-plans-different-sized-battery-cells-to-preserve-design-of-future-models (accessed 31 December, 2019).
[24] D. Phil. Honda e battery specs and platform revealed, 31,000 have 'expressed interest' in the electric car. Electrek. https://electrek.co/2019/06/13/honda-e-battery-platform/(accessed 31 December, 2019).
[25] G. Auto. Emgrand EV, Fashionably eco-feiendly. http://global.geely.com/car/emgrand-ev-2/(accessed 31 December, 2019).
[26] G. Renault. Zoe – the ultimate city car, designed for everyday practicality and convenience. https://group.renault.com/en/innovation-2/electric-vehicle/(accessed 31 December, 2019).
[27] B. Matt. Hyundai Kona electric 2019 review – Australia. Carsales. https://www.carsales.com.au/editorial/details/hyundai-kona-electric-2019-review-australia-117573/?&tracking=dsa&gclid=Cj0KCQiA0ZHwBRCRARIsAK0Tr-raGraRwr_h

AjJfiyhWKNIOluj3Y6XhBUFQbaibgZvklKXUFF05jVYaAiEYEALw_wcB&gclsrc=aw.ds (accessed 31 December, 2019).
[28] A. E. Paul. Exclusive: FCA has big news coming in electrification. The Detroit Bureau. https://www.thedetroitbureau.com/2019/06/exclusive-fca-has-big-news-coming-in-electrification/(accessed 31 December, 2019).
[29] Z. Rao, S. Wang, A review of power battery thermal energy management, Renew. Sustain. Energy Rev. 15 (9) (2011) 4554–4571.
[30] Q. Wang, B. Jiang, B. Li, Y. Yan, A critical review of thermal management models and solutions of lithium-ion batteries for the development of pure electric vehicles, Renew. Sustain. Energy Rev. 64 (2016) 106–128.
[31] Z. An, L. Jia, Y. Ding, C. Dang, X. Li, A review on lithium-ion power battery thermal management technologies and thermal safety, J. Therm. Sci. 26 (5) (2017) 391–412.
[32] G. Xia, L. Cao, G. Bi, A review on battery thermal management in electric vehicle application, J. Power Sources 367 (2017) 90–105.
[33] J. Kim, J. Oh, H. Lee, Review on battery thermal management system for electric vehicles, Appl. Therm. Eng. 149 (2019) 192–212.
[34] H. Liu, Z. Wei, W. He, J. Zhao, Thermal issues about Li-ion batteries and recent progress in battery thermal management systems: a review, Energy Convers. Manag. 150 (2017) 304–330.
[35] W. Wu, S. Wang, W. Wu, K. Chen, S. Hong, Y. Lai, A critical review of battery thermal performance and liquid based battery thermal management, Energy Convers. Manag. 182 (2019) 262–281.
[36] A.H. Akinlabi, D. Solyali, Configuration, design, and optimization of air-cooled battery thermal management system for electric vehicles: a review, Renew. Sustain. Energy Rev. 125 (2020) 109815.
[37] M.S. Islam, D.J. Driscoll, C.A. Fisher, P.R. Slater, Atomic-scale investigation of defects, dopants, and lithium transport in the LiFePO4 olivine-type battery material, Chem. Mater. 17 (20) (2005) 5085–5092.
[38] C. Daniel, D. Mohanty, J. Li, D.L. Wood, Cathode Materials Review, 2014.
[39] S.-L. Wu, W. Zhang, X. Song, A.K. Shukla, G. Liu, V. Battaglia, V. Srinivasan, High rate capability of Li (Ni1/3Mn1/3Co1/3) O2 electrode for Li-ion batteries, J. Electrochem. Soc. 159 (4) (2012) A438–A444.
[40] H.-J. Noh, S. Youn, C.S. Yoon, Y.-K. Sun, Comparison of the structural and electrochemical properties of layered Li [NixCoyMnz] O2 (x= 1/3, 0.5, 0.6, 0.7, 0.8 and 0.85) cathode material for lithium-ion batteries, J. Power Sources 233 (2013) 121–130.
[41] P. Kalyani, N. Kalaiselvi, Various aspects of LiNiO2chemistry: a review, Sci. Technol. Adv. Mater. 6 (6) (2016) 689–703.
[42] T.-F. Yi, Y.-R. Zhu, X.-D. Zhu, J. Shu, C.-B. Yue, A.-N. Zhou, A review of recent developments in the surface modification of LiMn2O4 as cathode material of power lithium-ion battery, Ionics 15 (6) (2009) 779–784.
[43] C. Forgez, D.V. Do, G. Friedrich, M. Morcrette, C. Delacourt, Thermal modeling of a cylindrical LiFePO4/graphite lithium-ion battery, J. Power Sources 195 (9) (2010) 2961–2968.
[44] W.-J. Zhang, Structure and performance of LiFePO4 cathode materials: a review, J. Power Sources 196 (6) (2011) 2962–2970.
[45] C. Täubert, M. Fleischhammer, M. Wohlfahrt-Mehrens, U. Wietelmann, T. Buhrmester, LiBOB as electrolyte salt or additive for lithium-ion batteries based on LiNi0. 8Co0. 15Al0. 05O2/graphite, J. Electrochem. Soc. 157 (6) (2010) A721–A728.
[46] D. Farhat, F. Ghamouss, J. Maibach, K. Edström, D. Lemordant, Adiponitrile–lithium bis (trimethylsulfonyl) imide solutions as Alkyl carbonate-free electrolytes for Li4Ti5O12 (LTO)/LiNi1/3Co1/3Mn1/3O2 (NMC) Li-ion batteries, ChemPhysChem 18 (10) (2017) 1333–1344.
[47] Q. Fan, S. Yang, J. Liu, H. Liu, K. Lin, R. Liu, C. Hong, L. Liu, Y. Chen, K. An, Mixed-conducting interlayer boosting the electrochemical performance of Ni-rich layered oxide cathode materials for lithium ion batteries, J. Power Sources 421 (2019) 91–99.
[48] Y. Jin, H. Yu, Y. Gao, X. He, T.A. White, X. Liang, Li4Ti5O12 coated with ultrathin aluminum-doped zinc oxide films as an anode material for lithium-ion batteries, J. Power Sources 436 (2019), 226859.
[49] M. Han, J. Yu, Subnanoscopically and homogeneously dispersed SiOx/C composite spheres for high-performance lithium ion battery anodes, J. Power Sources 414 (2019) 435–443.
[50] Y. Xiang, W. Zhang, B. Chen, Z. Jin, H. Zhang, P. Zhao, G. Cao, Q. Meng, Nano-Li4Ti5O12 particles in-situ deposited on compact holey-graphene framework for high volumetric power capability of lithium ion battery anode, J. Power Sources 447 (2020) 227372.
[51] M.E. Sotomayor, C. de La Torre-Gamarra, B. Levenfeld, J.-Y. Sanchez, A. Varez, G.-T. Kim, A. Varzi, S. Passerini, Ultra-thick battery electrodes for high gravimetric and volumetric energy density Li-ion batteries, J. Power Sources 437 (2019) 226923.
[52] D. Li, L. Chen, L. Chen, Q. Sun, M. Zhu, Y. Zhang, Y. Liu, Z. Liang, P. Si, J. Lou, Potassium gluconate-derived N/S Co-doped carbon nanosheets as superior electrode materials for supercapacitors and sodium-ion batteries, J. Power Sources 414 (2019) 308–316.
[53] X. Shi, Q. Sun, B. Boateng, Y. Niu, Y. Han, W. Lv, W. He, A quasi-solid composite separator with high ductility for safe and high-performance lithium-ion batteries, J. Power Sources 414 (2019) 225–232.
[54] J. Oh, H. Jo, H. Lee, H.-T. Kim, Y.M. Lee, M.-H. Ryou, Polydopamine-treated three-dimensional carbon fiber-coated separator for achieving high-performance lithium metal batteries, J. Power Sources 430 (2019) 130–136.
[55] J.R. Nair, F. Colò, A. Kazzazi, M. Moreno, D. Bresser, R. Lin, F. Bella, G. Meligrana, S. Fantini, E. Simonetti, Room temperature ionic liquid (RTIL)-based electrolyte cocktails for safe, high working potential Li-based polymer batteries, J. Power Sources 412 (2019) 398–407.
[56] B. Peng, Y. Li, J. Gao, F. Zhang, J. Li, G. Zhang, High energy K-ion batteries based on P3-Type K0· 5MnO2 hollow submicrosphere cathode, J. Power Sources 437 (2019), 226913.
[57] Y. Wang, P. Cui, W. Zhu, Z. Feng, M.-J. Vigeant, H. Demers, A. Guerfi, K. Zaghib, Enhancing the electrochemical performance of an O3–NaCrO2 cathode in sodium-ion batteries by cation substitution, J. Power Sources 435 (2019), 226760.
[58] J. Ming, J. Guo, C. Xia, W. Wang, H.N. Alshareef, Zinc-ion batteries: materials, mechanisms, and applications, Mater. Sci. Eng. R Rep. 135 (2019) 58–84.
[59] S. Chen, Y. Zhang, H. Geng, Y. Yang, X. Rui, C.C. Li, Zinc ions pillared vanadate cathodes by chemical pre-intercalation towards long cycling life and low-temperature zinc ion batteries, J. Power Sources 441 (2019), 227192.
[60] H. Xiao. Battery thermal management in electric vehicles. ANSYS. https://support.ansys.com/staticassets/ANSYS/staticassets/resourcelibrary/whitepaper/wp-battery-thermal-management.pdf (accessed 19 January, 2020).
[61] D. Bernardi, E. Pawlikowski, J. Newman, A general energy balance for battery systems, J. Electrochem. Soc. 132 (1) (1985) 5.
[62] Q. Norman. Industry developments in thermal management of electric vehicle batteries. Advanced Thermal Solutions. https://www.qats.com/cms/category/battery-cooling/(accessed 19 January, 2020).
[63] J. Gate, Rechargeable Batteries Applications Handbook, Newnes, Newton, 1998.
[64] K. Jalkanen, T. Aho, K. Vuorilehto, Entropy change effects on the thermal behavior of a LiFePO4/graphite lithium-ion cell at different states of charge, J. Power Sources 243 (2013) 354–360.
[65] X. Feng, H.B. Gooi, S.X. Chen, An improved lithium-ion battery model with temperature prediction considering entropy, in: 2012 3rd IEEE PES Innovative Smart Grid Technologies Europe (ISGT Europe), IEEE, 2012, pp. 1–8.
[66] J. Newman, K.E. Thomas-Alyea, Electrochemical Systems, John Wiley & Sons, 2012.
[67] Y. Xie, X.-j. He, X.-s. Hu, W. Li, Y.-j. Zhang, B. Liu, Y.-t. Sun, An improved resistance-based thermal model for a pouch lithium-ion battery considering heat generation of posts, Appl. Therm. Eng. 164 (2020), 114455.
[68] Y. Kobayashi, H. Miyashiro, K. Kumai, K. Takei, T. Iwahori, I. Uchida, Precise electrochemical calorimetry of LiCoO2/graphite lithium-ion cell: understanding thermal behavior and estimation of degradation mechanism, J. Electrochem. Soc. 149 (8) (2002) A978.
[69] K. Chen, G. Unsworth, X. Li, Measurements of heat generation in prismatic Li-ion batteries, J. Power Sources 261 (2014) 28–37.
[70] S. Drake, M. Martin, D. Wetz, J. Ostanek, S. Miller, J. Heinzel, A. Jain, Heat generation rate measurement in a Li-ion cell at large C-rates through temperature and heat flux measurements, J. Power Sources 285 (2015) 266–273.
[71] J. Zhang, J. Huang, Z. Li, B. Wu, Z. Nie, Y. Sun, F. An, N. Wu, Comparison and validation of methods for estimating heat generation rate of large-format lithium-ion batteries, J. Therm. Anal. Calorim. 117 (1) (2014) 447–461.
[72] B. Wu, Z. Li, J. Zhang, Thermal design for the pouch-type large-format lithium-ion batteries: I. Thermo-electrical modeling and origins of temperature non-uniformity, J. Electrochem. Soc. 162 (1) (2014) A181.
[73] E. Schuster, C. Ziebert, A. Melcher, M. Rohde, H.J. Seifert, Thermal behavior and electrochemical heat generation in a commercial 40 Ah lithium ion pouch cell, J. Power Sources 286 (2015) 580–589.
[74] Y. Saito, M. Shikano, H. Kobayashi, Heat generation behavior during charging and discharging of lithium-ion batteries after long-time storage, J. Power Sources 244 (2013) 294–299.
[75] Y. Ye, L.H. Saw, Y. Shi, A.A. Tay, Numerical analyses on optimizing a heat pipe thermal management system for lithium-ion batteries during fast charging, Appl. Therm. Eng. 86 (2015) 281–291.
[76] X. Xu, R. He, Review on the heat dissipation performance of battery pack with different structures and operation conditions, Renew. Sustain. Energy Rev. 29 (2014) 301–315.
[77] C. Wang, G. Zhang, L. Meng, X. Li, W. Situ, Y. Lv, M. Rao, Liquid cooling based on thermal silica plate for battery thermal management system, Int. J. Energy Res. 41 (15) (2017) 2468–2479.
[78] L. Sheng, L. Su, H. Zhang, Y. Fang, H. Xu, W. Ye, An improved calorimetric method for characterizations of the specific heat and the heat generation rate in a prismatic lithium ion battery cell, Energy Convers. Manag. 180 (2019) 724–732.
[79] Z.H. Wu Qingyu, Junwei Li, Calibrated calorimetry for measuring the specific heat capacityand heat generation rate of lithium-ion battery, Automot. Eng. 42 (1) (2020) 59–65.
[80] P. Ramadass, B. Haran, R. White, B.N. Popov, Capacity fade of Sony 18650 cells cycled at elevated temperatures: Part I. Cycling performance, J. Power Sources 112 (2) (2002) 606–613.
[81] P. Ramadass, B. Haran, R. White, B.N. Popov, Capacity fade of Sony 18650 cells cycled at elevated temperatures: Part II. Capacity fade analysis, J. Power Sources 112 (2) (2002) 614–620.
[82] A. Szumanowski, Y. Chang, Battery management system based on battery nonlinear dynamics modeling, IEEE Trans. Veh. Technol. 57 (3) (2008) 1425–1432.
[83] J. Belt, V. Utgikar, I. Bloom, Calendar and PHEV cycle life aging of high-energy, lithium-ion cells containing blended spinel and layered-oxide cathodes, J. Power Sources 196 (23) (2011) 10213–10221.
[84] D. Aurbach, Y. Talyosef, B. Markovsky, E. Markevich, E. Zinigrad, L. Asraf, J. S. Gnanaraj, H.-J. Kim, Design of electrolyte solutions for Li and Li-ion batteries: a review, Electrochim. Acta 50 (2–3) (2004) 247–254.

[85] R. Zhao, J. Liu, J. Gu, The effects of electrode thickness on the electrochemical and thermal characteristics of lithium ion battery, Appl. Energy 139 (2015) 220–229.
[86] J. Li, E. Murphy, J. Winnick, P. Kohl, Studies on the cycle life of commercial lithium ion batteries during rapid charge–discharge cycling, J. Power Sources 102 (1–2) (2001) 294–301.
[87] Q. Zhang, R.E. White, Capacity fade analysis of a lithium ion cell, J. Power Sources 179 (2) (2008) 793–798.
[88] Y. Kitagawa, K. Kato, M. Fukui, Analysis and experimentation for effective cooling of Li-ion batteries, Procedia Technology 18 (2014) 63–67.
[89] W. Waag, S. Käbitz, D.U. Sauer, Experimental investigation of the lithium-ion battery impedance characteristic at various conditions and aging states and its influence on the application, Appl. Energy 102 (2013) 885–897.
[90] S. Saxena, C. Hendricks, M. Pecht, Cycle life testing and modeling of graphite/LiCoO2 cells under different state of charge ranges, J. Power Sources 327 (2016) 394–400.
[91] L. Su, J. Zhang, C. Wang, Y. Zhang, Z. Li, Y. Song, T. Jin, Z. Ma, Identifying main factors of capacity fading in lithium ion cells using orthogonal design of experiments, Appl. Energy 163 (2016) 201–210.
[92] M.M. Kabir, D.E. Demirocak, Degradation mechanisms in Li-ion batteries: a state-of-the-art review, Int. J. Energy Res. 41 (14) (2017) 1963–1986.
[93] D. Li, D.L. Danilov, H.J. Bergveld, R.-A. Eichel, P.H. Notten, Understanding battery aging mechanisms, in: Future Lithium-Ion Batteries, 2019, pp. 220–250.
[94] K. Smith, E. Wood, S. Santhanagopalan, G. Kim, A. Pesaran, Advanced models and controls for prediction and extension of battery lifetime, in: Advanced Automotive Battery Conference, Atlanta, GA, 2014, pp. 4–6.
[95] F. Leng, C.M. Tan, M. Pecht, Effect of temperature on the aging rate of Li ion battery operating above room temperature, Sci. Rep. 5 (2015) 12967.
[96] H. Gabrisch, Y. Ozawa, R. Yazami, Crystal structure studies of thermally aged LiCoO2 and LiMn2O4 cathodes, Electrochim. Acta 52 (4) (2006) 1499–1506.
[97] X. Zhou, J. Huang, Z. Pan, M. Ouyang, Impedance characterization of lithium-ion batteries aging under high-temperature cycling: importance of electrolyte-phase diffusion, J. Power Sources 426 (2019) 216–222.
[98] Z. Tang, S. Wang, Z. Liu, J. Cheng, Numerical analysis of temperature uniformity of a liquid cooling battery module composed of heat-conducting blocks with gradient contact surface angles, Appl. Therm. Eng. 178 (2020) 115509.
[99] P. Ni, X. Wang, Temperature field and temperature difference of a battery package for a hybrid car, Case Stud. Therm. Eng. (2020) 100646.
[100] A.A. Pesaran, Battery thermal models for hybrid vehicle simulations, J. Power Sources 110 (2) (2002) 377–382.
[101] C. Park, A.K. Jaura, Dynamic Thermal Model of Li-Ion Battery for Predictive Behavior in Hybrid and Fuel Cell Vehicles, SAE Technical Paper, 0148-7191, 2003.
[102] Z. Rao, S. Wang, G. Zhang, Simulation and experiment of thermal energy management with phase change material for ageing LiFePO4 power battery, Energy Convers. Manag. 52 (12) (2011) 3408–3414.
[103] H. Park, A design of air flow configuration for cooling lithium ion battery in hybrid electric vehicles, J. Power Sources 239 (2013) 30–36.
[104] L. Panasonic, Co. *Lithium Ion NCR18650PF*, 2016, June, p. 31 [Online]. Available, https://www.omnitron.cz/download/datasheet/NCR-18650PF.pdf. (Accessed December 2019).
[105] X.-H. Yang, S.-C. Tan, J. Liu, Thermal management of Li-ion battery with liquid metal 117, Energy Conversion and Management, 2016, pp. 577–585.
[106] A. Schmidt, A. Smith, H. Ehrenberg, Power capability and cyclic aging of commercial, high power lithium ion battery cells with respect to different cell designs, J. Power Sources 425 (2019) 27–38.
[107] Q. Wang, P. Ping, X. Zhao, G. Chu, J. Sun, C. Chen, Thermal runaway caused fire and explosion of lithium ion battery, J. Power Sources 208 (2012) 210–224.
[108] S. Arora, W. Shen, A. Kapoor, Review of mechanical design and strategic placement technique of a robust battery pack for electric vehicles, Renew. Sustain. Energy Rev. 60 (2016) 1319–1331.
[109] V. Ruiz, A. Pfrang, A. Kriston, N. Omar, P. Van den Bossche, L. Boon-Brett, A review of international abuse testing standards and regulations for lithium ion batteries in electric and hybrid electric vehicles, Renew. Sustain. Energy Rev. 81 (2018) 1427–1452.
[110] A.W. Golubkov, D. Fuchs, J. Wagner, H. Wiltsche, C. Stangl, G. Fauler, G. Voitic, A. Thaler, V. Hacker, Thermal-runaway experiments on consumer Li-ion batteries with metal-oxide and olivin-type cathodes, RSC Adv. 4 (7) (2014) 3633–3642.
[111] H.M. Barkholtz, Y. Preger, S. Ivanov, J. Langendorf, L. Torres-Castro, J. Lamb, B. Chalamala, S.R. Ferreira, Multi-scale thermal stability study of commercial lithium-ion batteries as a function of cathode chemistry and state-of-charge, J. Power Sources 435 (2019) 226777.
[112] S. Hossain, Y.-K. Kim, Y. Saleh, R. Loutfy, Overcharge studies of carbon fiber composite-based lithium-ion cells, J. Power Sources 161 (1) (2006) 640–647.
[113] E. Roth, D. Doughty, D. Pile, Effects of separator breakdown on abuse response of 18650 Li-ion cells, J. Power Sources 174 (2) (2007) 579–583.
[114] C.L. Campion, W. Li, B.L. Lucht, Thermal decomposition of LiPF6-based electrolytes for lithium-ion batteries, J. Electrochem. Soc. 152 (12) (2005) A2327–A2334.
[115] N.P. Lebedeva, F.D. Persio, T. Kosmidou, D. Dams, A. Pfrang, A. Kersys, L. Boon-Brett, Amount of free liquid electrolyte in commercial large format prismatic Li-ion battery cells, J. Electrochem. Soc. 166 (4) (2019) A779–A786.
[116] V. Peter, GM Recalls Volts to Fix Fire Risk, The Comeback of the American Car, CNN Money, 2012.
[117] R. Charles, Tesla Dodges Full Investigation after Fiery Crash, CNN Money, Hongkong, 2013.
[118] A. Pfrang, A. Kriston, V. Ruiz, N. Lebedeva, F. Di Persio, Safety of rechargeable energy storage systems with a focus on Li-ion technology, in: Emerging Nanotechnologies in Rechargeable Energy Storage Systems, Elsevier, 2017, pp. 253–290.
[119] X. Feng, S. Zheng, D. Ren, X. He, L. Wang, H. Cui, X. Liu, C. Jin, F. Zhang, C. Xu, Investigating the thermal runaway mechanisms of lithium-ion batteries based on thermal analysis database, Appl. Energy 246 (2019) 53–64.
[120] X. Feng, D. Ren, X. He, M. Ouyang, Mitigating Thermal Runaway of Lithium-Ion Batteries, Joule, 2020.
[121] D.H. Doughty, E.P. Roth, A general discussion of Li ion battery safety, The Electrochemical Society Interface 21 (2) (2012) 37–44.
[122] Y.S. Choi, D.M. Kang, Prediction of thermal behaviors of an air-cooled lithium-ion battery system for hybrid electric vehicles, J. Power Sources 270 (2014) 273–280.
[123] Q. Wang, X. Zhao, J. Ye, Q. Sun, P. Ping, J. Sun, Thermal response of lithium-ion battery during charging and discharging under adiabatic conditions, J. Therm. Anal. Calorim. 124 (1) (2016) 417–428.
[124] A.A. Pesaran, Battery thermal management in EV and HEVs: issues and solutions, Battery Man. 43 (5) (2001) 34–49.
[125] K. Kelly, J. Rugh, A. Pesaran, Improving battery thermal management using design for six sigma process, in: For Presentation at the 20 th Electric Vehicle Symposium, Long Beach, CA November 15-18, 2003, 2003.
[126] Y. Ye, Y. Shi, N. Cai, J. Lee, X. He, Electro-thermal modeling and experimental validation for lithium ion battery, J. Power Sources 199 (2012) 227–238.
[127] L. Lu, X. Han, J. Li, J. Hua, M. Ouyang, A review on the key issues for lithium-ion battery management in electric vehicles, J. Power Sources 226 (2013) 272–288.
[128] J. Jaguemont, L. Boulon, Y. Dubé, A comprehensive review of lithium-ion batteries used in hybrid and electric vehicles at cold temperatures, Appl. Energy 164 (2016) 99–114.
[129] R. Koyama, Y. Arai, Y. Yamauchi, S. Takeya, F. Endo, A. Hotta, R. Ohmura, Thermophysical properties of trimethylolethane (TME) hydrate as phase change material for cooling lithium-ion battery in electric vehicle, J. Power Sources 427 (2019) 70–76.
[130] J. Chen, S. Kang, E. Jiaqiang, Z. Huang, K. Wei, B. Zhang, H. Zhu, Y. Deng, F. Zhang, G. Liao, Effects of different phase change material thermal management strategies on the cooling performance of the power lithium ion batteries: a review, J. Power Sources 442 (2019) 227228.
[131] R. Zhao, S. Zhang, J. Liu, J. Gu, A review of thermal performance improving methods of lithium ion battery: electrode modification and thermal management system, J. Power Sources 299 (2015) 557–577.
[132] D. Chen, J. Jiang, G.-H. Kim, C. Yang, A. Pesaran, Comparison of different cooling methods for lithium ion battery cells, Appl. Therm. Eng. 94 (2016) 846–854.
[133] R. Kizilel, R. Sabbah, J.R. Selman, S. Al-Hallaj, An alternative cooling system to enhance the safety of Li-ion battery packs, J. Power Sources 194 (2) (2009) 1105–1112.
[134] M.H. Westbrook, M. Westbrook, The Electric Car: Development and Future of Battery, Hybrid and Fuel-Cell Cars, Iet 38, 2001.
[135] M. Arasu, Q. Ahmed, G. Rizzoni, Optimizing Battery Cooling System for a Range Extended Electric Truck, SAE Technical Paper, 0148-7191, 2019.
[136] S. Park, D. Jung, Battery cell arrangement and heat transfer fluid effects on the parasitic power consumption and the cell temperature distribution in a hybrid electric vehicle, J. Power Sources 227 (2013) 191–198.
[137] M.R. Giuliano, A.K. Prasad, S.G. Advani, Experimental study of an air-cooled thermal management system for high capacity lithium–titanate batteries, J. Power Sources 216 (2012) 345–352.
[138] A. Pesaran, G. Kim, Battery Thermal Management System Design Modeling, National Renewable Energy Lab.(NREL), Golden, CO (United States), 2006.
[139] K.J. Kelly, M. Mihalic, M. Zolot, Battery usage and thermal performance of the Toyota Prius and Honda Insight during chassis dynamometer testing, in: Seventeenth Annual Battery Conference on Applications and Advances. Proceedings of Conference (Cat. No. 02TH8576), IEEE, 2002, pp. 247–252.
[140] A. Pesaran, M. Keyser, S. Burch, An Approach for Designing Thermal Management Systems for Electric and Hybrid Vehicle Battery Packs, National Renewable Energy Laboratory, Golden, CO (US), 1999.
[141] Volkswagen E-up! Air cooled battery, featured in ViaVision magazine. My electric car forums. https://www.myelectriccarforums.com/volkswagen-e-up-air-cooled-battery-featured-in-viavision-magazine/(accessed 19 January, 2020).
[142] L. Andrew. Volkswagen's EV racecar just broke records during this year's Pikes Peak Hill Climb. The Verge. https://www.theverge.com/2018/6/24/17078544/volkswagen-ev-race-car-pikes-peak-hill-climb-record (accessed 19 January, 2020).
[143] D. G. Marcus. Lexus' first-ever electric vehicle is the UX300e. Autoindustriya. https://www.autoindustriya.com/auto-industry-news/lexus-first-ever-electric-vehicle-is-the-ux300e.html (accessed 20 January, 2020).
[144] L. Eric. Here's why nissan employs active air cooling in e-NV200 battery pack. InsideEVs. https://insideevs.com/news/322347/heres-why-nissan-employs-active-air cooling-in-e-nv200-battery-pack/(accessed 20 January, 2020).
[145] P. Rodgers, V. Eveloy, M.G. Pecht, Limits of air cooling: status and challenges, in: Semiconductor Thermal Measurement and Management IEEE Twenty First Annual IEEE Symposium, IEEE, 2005, pp. 116–124.
[146] R. Jilte, R. Kumar, Numerical investigation on cooling performance of Li-ion battery thermal management system at high galvanostatic discharge, Eng. Sci. Technology. Int. J. 21 (5) (2018) 957–969.
[147] C.-W. Park, A.K. Jaura, Thermal Analysis of Cooling System in Hybrid Electric Vehicles, SAE Technical Paper, 0148-7191, 2002.

[148] T. Wang, K.J. Tseng, J. Zhao, Development of efficient air cooling strategies for lithium-ion battery module based on empirical heat source model, Appl. Therm. Eng. 90 (2015) 521–529.
[149] D.C. Erb, S. Kumar, S.E. Sarma, E. Carlson, Size matters: why cell size is vital for minimizing cost of air cooling in battery packs, in: 2015 IEEE Transportation Electrification Conference and Expo (ITEC), IEEE, 2015, pp. 1–6.
[150] T. Wang, K.J. Tseng, J. Zhao, Z. Wei, Thermal investigation of lithium-ion battery module with different cell arrangement structures and forced air cooling strategies, Appl. Energy 134 (2014) 229–238.
[151] D. Kang, P.-Y. Lee, K. Yoo, J. Kim, Internal thermal network model-based inner temperature distribution of high-power lithium-ion battery packs with different shapes for thermal management, J. Energy Stor. vol. 27, 2020.
[152] Y. Zhang, X. Song, C. Ma, D. Hao, Y. Chen, Effects of the structure arrangement and spacing on the thermal characteristics of Li-ion battery pack at various discharge rates, Appl. Therm. Eng. 165 (2020).
[153] N. Yang, X. Zhang, G. Li, D. Hua, Assessment of the forced air cooling performance for cylindrical lithium-ion battery packs: a comparative analysis between aligned and staggered cell arrangements, Appl. Therm. Eng. 80 (2015) 55–65.
[154] Y. Fan, Y. Bao, C. Ling, Y. Chu, X. Tan, S. Yang, Experimental study on the thermal management performance of air cooling for high energy density cylindrical lithium-ion batteries, Appl. Therm. Eng. 155 (2019) 96–109.
[155] M. Ye, Y. Xu, Y. Huangfu, The structure optimization of lithium-ion battery pack based on fluid-solid conjugate thermodynamic analysis, Energy Procedia 152 (2018) 643–648.
[156] K. Chen, S. Wang, M. Song, L. Chen, Configuration optimization of battery pack in parallel air-cooled battery thermal management system using an optimization strategy, Appl. Therm. Eng. 123 (2017) 177–186.
[157] T. Yang, N. Yang, X. Zhang, G. Li, Investigation of the thermal performance of axial-flow air cooling for the lithium-ion battery pack, Int. J. Therm. Sci. 108 (2016) 132–144.
[158] X. Yu, Z. Lu, L. Zhang, L. Wei, X. Cui, L. Jin, Experimental study on transient thermal characteristics of stagger-arranged lithium-ion battery pack with air cooling strategy, Int. J. Heat Mass Tran. 143 (2019) 118576.
[159] B. Severino, F. Gana, R. Palma-Behnke, P.A. Estévez, W.R. Calderón-Muñoz, M. E. Orchard, J. Reyes, M. Cortés, Multi-objective optimal design of lithium-ion battery packs based on evolutionary algorithms, J. Power Sources 267 (2014) 288–299.
[160] W. Li, M. Xiao, X. Peng, A. Garg, L. Gao, A surrogate thermal modeling and parametric optimization of battery pack with air cooling for EVs, Appl. Therm. Eng. 147 (2019) 90–100.
[161] L. Fan, J.M. Khodadadi, A.A. Pesaran, A parametric study on thermal management of an air-cooled lithium-ion battery module for plug-in hybrid electric vehicles, J. Power Sources 238 (2013) 301–312.
[162] J. Xun, R. Liu, K. Jiao, Numerical and analytical modeling of lithium ion battery thermal behaviors with different cooling designs, J. Power Sources 233 (2013) 47–61.
[163] X.M. Xu, R. He, Research on the heat dissipation performance of battery pack based on forced air cooling, J. Power Sources 240 (2013) 33–41.
[164] H. Sun, R. Dixon, Development of cooling strategy for an air cooled lithium-ion battery pack, J. Power Sources 272 (2014) 404–414.
[165] K. Chen, M. Song, W. Wei, S. Wang, Structure optimization of parallel air-cooled battery thermal management system with U-type flow for cooling efficiency improvement, Energy 145 (2018) 603–613.
[166] Z. Lu, X. Yu, L. Wei, Y. Qiu, L. Zhang, X. Meng, L. Jin, Parametric study of forced air cooling strategy for lithium-ion battery pack with staggered arrangement, Appl. Therm. Eng. 136 (2018) 28–40.
[167] Y. Liu, J. Zhang, Design a J-type air-based battery thermal management system through surrogate-based optimization, Appl. Energy 252 (2019).
[168] K. Yu, X. Yang, Y. Cheng, C. Li, Thermal analysis and two-directional air flow thermal management for lithium-ion battery pack, J. Power Sources 270 (2014) 193–200.
[169] H. Fathabadi, A novel design including cooling media for Lithium-ion batteries pack used in hybrid and electric vehicles, J. Power Sources 245 (2014) 495–500.
[170] H. Zhou, F. Zhou, L. Xu, J. Kong, QingxinYang, Thermal performance of cylindrical Lithium-ion battery thermal management system based on air distribution pipe, Int. J. Heat Mass Tran. 131 (2019) 984–998.
[171] Z. Lu, X.Z. Meng, L.C. Wei, W.Y. Hu, L.Y. Zhang, L.W. Jin, Thermal management of densely-packed EV battery with forced air cooling strategies, Energy Procedia 88 (2016) 682–688.
[172] H. Wang, L. Ma, Thermal management of a large prismatic battery pack based on reciprocating flow and active control, Int. J. Heat Mass Tran. 115 (2017) 296–303.
[173] X. Na, H. Kang, T. Wang, Y. Wang, Reverse layered air flow for Li-ion battery thermal management, Appl. Therm. Eng. 143 (2018) 257–262.
[174] M. Soltani, G. Berckmans, J. Jaguemont, J. Ronsmans, S. Kakihara, O. Hegazy, J. Van Mierlo, N. Omar, Three dimensional thermal model development and validation for lithium-ion capacitor module including air cooling system, Appl. Therm. Eng. 153 (2019) 264–274.
[175] J. Zhao, Z. Rao, Y. Li, Thermal performance of mini-channel liquid cooled cylinder based battery thermal management for cylindrical lithium-ion power battery, Energy Convers. Manag. 103 (2015) 157–165.
[176] K. Chen, W. Wu, F. Yuan, L. Chen, S. Wang, Cooling efficiency improvement of air-cooled battery thermal management system through designing the flow pattern, Energy 167 (2019) 781–790.
[177] K. Chen, Y. Chen, Y. She, M. Song, S. Wang, L. Chen, Construction of effective symmetrical air-cooled system for battery thermal management, Appl. Therm. Eng. 166 (2020) 114679.
[178] Y.-W. Wang, J.-M. Jiang, Y.-H. Chung, W.-C. Chen, C.-M. Shu, Forced-air cooling system for large-scale lithium-ion battery modules during charge and discharge processes, J. Therm. Anal. Calorim. 135 (5) (2018) 2891–2901.
[179] J. E, M. Yue, J. Chen, H. Zhu, Y. Deng, Y. Zhu, F. Zhang, M. Wen, B. Zhang, S. Kang, Effects of the different air cooling strategies on cooling performance of a lithium-ion battery module with baffle, Appl. Therm. Eng. 144 (2018) 231–241.
[180] S. Shahid, M. Agelin-Chaab, Experimental and numerical studies on air cooling and temperature uniformity in a battery pack, Int. J. Energy Res. 42 (6) (2018) 2246–2262.
[181] S. Shahid, M. Agelin-Chaab, Analysis of cooling effectiveness and temperature uniformity in a battery pack for cylindrical batteries, Energies 10 (8) (2017) 1157.
[182] K. Chen, Z. Li, Y. Chen, S. Long, J. Hou, M. Song, S. Wang, Design of parallel air-cooled battery thermal management system through numerical study, Energies 10 (10) (2017).
[183] S. Hong, X. Zhang, K. Chen, S. Wang, Design of flow configuration for parallel air-cooled battery thermal management system with secondary vent, Int. J. Heat Mass Tran. 116 (2018) 1204–1212.
[184] C. Zhu, X. Li, L. Song, L. Xiang, Development of a theoretically based thermal model for lithium ion battery pack, J. Power Sources 223 (2013) 155–164.
[185] L.H. Saw, Y. Ye, M.C. Yew, W.T. Chong, M.K. Yew, T.C. Ng, Computational fluid dynamics simulation on open cell aluminium foams for Li-ion battery cooling system, Appl. Energy 204 (2017) 1489–1499.
[186] X. Li, F. He, G. Zhang, Q. Huang, D. Zhou, Experiment and simulation for pouch battery with silica cooling plates and copper mesh based air cooling thermal management system, Appl. Therm. Eng. 146 (2019) 866–880.
[187] S.K. Mohammadian, S.M. Rassoulinejad-Mousavi, Y. Zhang, Thermal management improvement of an air-cooled high-power lithium-ion battery by embedding metal foam, J. Power Sources 296 (2015) 305–313.
[188] S.K. Mohammadian, Y. Zhang, Cumulative effects of using pin fin heat sink and porous metal foam on thermal management of lithium-ion batteries, Appl. Therm. Eng. 118 (2017) 375–384.
[189] R.D. Jilte, R. Kumar, M.H. Ahmadi, L. Chen, Battery thermal management system employing phase change material with cell-to-cell air cooling, Appl. Therm. Eng. 161 (2019).
[190] P. Qin, M. Liao, D. Zhang, Y. Liu, J. Sun, Q. Wang, Experimental and numerical study on a novel hybrid battery thermal management system integrated forced-air convection and phase change material, Energy Convers. Manag. 195 (2019) 1371–1381.
[191] M. Mehrabi-Kermani, E. Houshfar, M. Ashjaee, A novel hybrid thermal management for Li-ion batteries using phase change materials embedded in copper foams combined with forced-air convection, Int. J. Therm. Sci. 141 (2019) 47–61.
[192] W. Luo, F. He, Q. Huang, X. Li, G. Zhang, Z. Zhong, Experimental investigation on thermal performance of silica cooling plate-aluminate thermal plate-coupled forced convection-based pouch battery thermal management system, Int. J. Energy Res. 43 (13) (2019) 7604–7613.
[193] L.H. Saw, H.M. Poon, H.S. Thiam, Z. Cai, W.T. Chong, N.A. Pambudi, Y.J. King, Novel thermal management system using mist cooling for lithium-ion battery packs, Appl. Energy 223 (2018) 146–158.
[194] A.M. Sefidan, A. Sojoudi, S.C. Saha, Nanofluid-based cooling of cylindrical lithium-ion battery packs employing forced air flow, Int. J. Therm. Sci. 117 (2017) 44–58.
[195] R. Zhao, J. Liu, J. Gu, L. Zhai, F. Ma, Experimental study of a direct evaporative cooling approach for Li-ion battery thermal management, Int. J. Energy Res. (2020).
[196] S.K. Mohammadian, Y. Zhang, Thermal management optimization of an air-cooled Li-ion battery module using pin-fin heat sinks for hybrid electric vehicles, J. Power Sources 273 (2015) 431–439.
[197] D. Dan, C. Yao, Y. Zhang, H. Zhang, Z. Zeng, X. Xu, Dynamic thermal behavior of micro heat pipe array-air cooling battery thermal management system based on thermal network model, Appl. Therm. Eng. 162 (2019).
[198] T. Han, B. Khalighi, E.C. Yen, S. Kaushik, Li-ion battery pack thermal management: liquid versus air cooling, J. Therm. Sci. Eng. Appl. 11 (2) (2019).
[199] W. Li, A. Jishnu, A. Garg, M. Xiao, X. Peng, L. Gao, Heat transfer efficiency enhancement of lithium-ion battery packs by using novel design of herringbone fins, J. Electrochem. Energy Convers. Stor. 17 (2) (2020).
[200] Y. Wei, M. Agelin-Chaab, Development and experimental analysis of a hybrid cooling concept for electric vehicle battery packs, J. Energy Stor. 25 (2019) 100906.
[201] Y. Zhao, Y. Patel, T. Zhang, G.J. Offer, Modeling the effects of thermal gradients induced by tab and surface cooling on lithium ion cell performance, J. Electrochem. Soc. 165 (13) (2018) A3169.
[202] I.A. Hunt, Y. Zhao, Y. Patel, G. Offer, Surface cooling causes accelerated degradation compared to tab cooling for lithium-ion pouch cells, J. Electrochem. Soc. 163 (9) (2016) A1846.
[203] O. Dondelewski, T.S. O'Connor, Y. Zhao, I.A. Hunt, A. Holland, A. Hales, G. J. Offer, Y. Patel, The role of cell geometry when selecting tab or surface cooling to minimise cell degradation, eTransportation 5 (2020) 100073.
[204] S. Li, N. Kirkaldy, C. Zhang, K. Gopalakrishnan, T. Amietszajew, L.B. Diaz, J. V. Barreras, M. Shams, X. Hua, Y. Patel, Optimal cell tab design and cooling strategy for cylindrical lithium-ion batteries, J. Power Sources 492 (2021), 229594.

[205] H. Heimes, A. Kampker, A. Mohsseni, F. Maltoni, J. Biederbeck, Cell tab cooling system for battery life extension, in: 2019 18th IEEE Intersociety Conference on Thermal and Thermomechanical Phenomena in Electronic Systems (ITherm), IEEE, 2019, pp. 1125–1133.
[206] M.S. Patil, J.-H. Seo, M.-Y. Lee, A novel dielectric fluid immersion cooling technology for Li-ion battery thermal management, Energy Convers. Manag. 229 (2021) 113715.
[207] J.-C. Jang, S.-H. Rhi, Battery thermal management system of future electric vehicles with loop thermosyphon, in: US-Korea Conference on Science, Technology, and Entrepreneurship, UKC), 2010.
[208] P. Gupta, S. Vardhan, Optimizing OEE, productivity and production cost for improving sales volume in an automobile industry through TPM: a case study, Int. J. Prod. Res. 54 (10) (2016) 2976–2988.
[209] A. Brooker, M. Thornton, J. Rugh, Technology Improvement Pathways to Cost-Effective Vehicle Electrification, 2010.
[210] R.J. Orsato, P. Wells, U-turn: the rise and demise of the automobile industry, J. Clean. Prod. 15 (11–12) (2007) 994–1006.
[211] K. Kisu, S. Kim, H. Oguchi, N. Toyama, S.-i. Orimo, Interfacial stability between LiBH4-based complex hydride solid electrolytes and Li metal anode for all-solid-state Li batteries, J. Power Sources 436 (2019) 226821.
[212] Y. Zhang, W. Lu, L. Cong, J. Liu, L. Sun, A. Mauger, C.M. Julien, H. Xie, J. Liu, Cross-linking network based on Poly (ethylene oxide): solid polymer electrolyte for room temperature lithium battery, J. Power Sources 420 (2019) 63–72.
[213] B. Zhang, L. Chen, J. Hu, Y. Liu, Y. Liu, Q. Feng, G. Zhu, L.-Z. Fan, Solid-state lithium metal batteries enabled with high loading composite cathode materials and ceramic-based composite electrolytes, J. Power Sources 442 (2019) 227230.
[214] H. Nguyen, A. Banerjee, X. Wang, D. Tan, E.A. Wu, J.-M. Doux, R. Stephens, G. Verbist, Y.S. Meng, Single-step synthesis of highly conductive Na3PS4 solid electrolyte for sodium all solid-state batteries, J. Power Sources 435 (2019) 126623.